

**This dissertation has been  
microfilmed exactly as received**

**70-9997**

**LEWIS, John Maurice, 1939-  
NUMERICAL VARIATIONAL OBJECTIVE  
ANALYSIS OF THE PLANETARY BOUNDARY  
LAYER IN CONJUNCTION WITH SQUALL LINE  
FORMATION.**

**The University of Oklahoma, Ph.D., 1970  
Physics, meteorology**

**University Microfilms, Inc., Ann Arbor, Michigan**

THE UNIVERSITY OF OKLAHOMA

GRADUATE COLLEGE

NUMERICAL VARIATIONAL OBJECTIVE ANALYSIS

OF THE

PLANETARY BOUNDARY LAYER

IN CONJUNCTION WITH SQUALL LINE FORMATION

A DISSERTATION

SUBMITTED TO THE GRADUATE FACULTY

in partial fulfillment of the requirements for

the degree of

DOCTOR OF PHILOSOPHY

BY

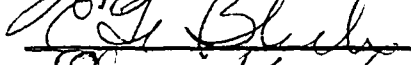
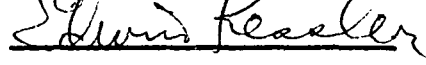
JOHN MAURICE LEWIS

Norman, Oklahoma

1969

NUMERICAL VARIATIONAL OBJECTIVE ANALYSIS  
OF THE  
PLANETARY BOUNDARY LAYER  
IN CONJUNCTION WITH SQUALL LINE FORMATION

APPROVED BY

  
\_\_\_\_\_  
  
\_\_\_\_\_  
  
\_\_\_\_\_

  
\_\_\_\_\_

DISSERTATION COMMITTEE

## DEDICATION

To my dearly loved sister, Maureen Ann, whose charity will  
live forever in those who knew her.

Charity suffereth long,  
and is kind; charity envieth  
not; charity vaunteth not  
itself, is not puffed up,

Doth not behave itself  
unseemly, seeketh not her  
own, is not easily  
provoked, thinketh no  
evil;

Rejoiceth not in iniquity,  
but rejoiceth in the truth;

Beareth all things,  
believeth all things, hopeth  
all things, endureth all  
things.

I Cor. 13:4-7

## ACKNOWLEDGEMENTS

Professor Sasaki deserves credit both as a scientific advisor and personal counselor. His enthusiasm for atmospheric investigation and his versatility with the tools of research have provided an excellent source of technical assistance and scientific inspiration. Encouragement and financial assistance to visit both the National Meteorological Center and the National Center for Atmospheric Research came from Professor Sasaki. These visits were stimulating and, moreover, the technical facilities at these installations were necessary for completion of the research.

Three government organizations and their personnel were vital to this research effort: (1) Development Division of NMC. Dr. Shuman, Director, made possible my summer, 1968 visit to NMC. Lt. Col. James Howcroft and Maj. Armand Desmarais provided the programming skill necessary to obtain data for the case study. Dr. John Stackpole and Mr. Ken Campana helped me obtain the information on the topography and drag coefficients. Also, while visiting NMC, the discussion with Dr. K. Miyakoda, Geophysical Fluid Dynamics Laboratory, was sincerely appreciated; (2) The National Severe Storms Laboratory. Dr. Edwin Kessler, Director, has encouraged this effort from the viewpoint of a doctoral committee member and coordinator of the sponsoring contract; (3) National Center for Atmospheric Research. The computer staff, especially Mr. David Robertson, Mr. Paul

Schwartztrauber, Mike Majors, and Janet Ivarie, gave valuable advice in connection with programming for the CDC 6600 at NCAR.

Those fellow students who are always willing to discuss research results and help in more mundane tasks such as hunting for program "bugs", contributed immeasurably. In this connection, special thanks are due Chuck Dowell, Buddy Ritchie, and Joe Cunningham. Lt. Jim Harris, while studying at the University of Oklahoma, willingly helped extract moisture information from the radiosonde records. Appreciation is expressed to Marcia Rucker, Keven Amrein, and Jan Stone for typing of the manuscript and to Mr. Carlos Driescher for drafting the figures.

TABLE OF CONTENTS

	Page
LIST OF TABLES.....	vii
LIST OF ILLUSTRATIONS.....	viii
ABSTRACT.....	ix
CHAPTER	
I. INTRODUCTION.....	1
II. METHOD OF OBJECTIVE ANALYSIS.....	5
III. APPLICATION TO A CASE OF SQUALL LINE FORMATION.....	15
IV. CONCLUSIONS AND REMARKS.....	24
BIBLIOGRAPHY.....	26
APPENDICES	
A. GOVERNING HYDRODYNAMICAL EQUATIONS.....	29
B. CONVERGENCE OF ITERATION SCHEME.....	44

LIST OF TABLES

Table		Page
1.	Operators in amplification matrix.....	49

LIST OF ILLUSTRATIONS

Illustration	Page
1. Topographic features over the network.....	50
2. Contours of the drag coefficient over the network.....	51
3. Coordinate surfaces in the vertical.....	52
4. The horizontal net of grid points and location of radiosonde stations.....	53
5. Spectral radius of the amplification matrix.....	54
6. Standard deviations of $u$ , $v$ , $\theta$ , and $q$ .....	55
7. Distribution of the severe storm index in relation to observed severe weather at 00 GMT, June 10.....	56
8. Distribution of the severe storm index in relation to observed severe weather at 03 GMT, June 10.....	57
9. Distribution of the severe storm index in relation to observed severe weather at 06 GMT, June 10.....	58
10. Distribution of specific humidity at 00 GMT, June 10.....	59
11. Distribution of specific humidity at 03 GMT, June 10.....	60
12. Distribution of specific humidity at 06 GMT, June 10.....	61
13. ESSA-5 satellite photographs on June 9, 1968.....	62
14. ESSA-5 satellite photographs on June 10, 1968.....	63

## ABSTRACT

Initial values of wind, temperature, pressure, and moisture are objectively determined for use in a boundary layer forecast model. The objective analysis is accomplished by using Sasaki's (1969) numerical variational method. This technique incorporates the governing thermo-hydrodynamical equations, as well as observations, into the initialization process. The solution to four coupled elliptic differential equations with associated boundary conditions completely determines the initial map. Richardson's relaxation method is used to solve the elliptic system.

The analysis and prediction is applied to severe weather occurrence in the Midwest on June 10, 1968. A 2 km thick layer bounded by the earth's surface and encompassing a horizontal area of approximately  $2000 \times 2000 \text{ km}^2$  is used. The horizontal grid spacing is 190 km and the vertical interval is 200 m. Data from the radiosonde network and the NMC analysis are used in conjunction with the governing equations to generate the initial fields. The 3 and 6 hr forecasts of a severe storm index,  $wq$ , are discussed. The areal distribution of this index, the product of vertical velocity and specific humidity, is compared with the surface observation of severe weather.

NUMERICAL VARIATIONAL OBJECTIVE ANALYSIS  
OF THE  
PLANETARY BOUNDARY LAYER  
IN CONJUNCTION WITH SQUALL LINE FORMATION

CHAPTER I

INTRODUCTION

In order to integrate the governing equations for atmospheric flow, initial ( $t = 0$ ) conditions for all meteorological variables in the model must be specified. Observations are the obvious source of information for these initial fields. The observations, however, contain information related to all possible scales of atmospheric motion detectable by the instrumentation. Since the atmospheric model is designed for a particular space and time scale, use of unmodified observations generally admits "noise" into the meteorological fields. That is, scales of motion appearing in the observations but unaccountable in the model contribute to the initial map. This contribution is termed noise and can eventually lead to forecast errors.

Hinkelmann (1951) investigated theoretically the problem of initialization when forecasting with the "primitive equations" (the Eulerian hydrodynamical equations modified by the assumption of hydrostatic balance). He showed that the amplitude of the high frequency gravity-inertia waves can be made smaller (by a factor of 10 in his model) than that of the desired

low frequency motion by using geostrophic values for the initial wind field.

The Joint Numerical Prediction Unit (JNWP; the forerunner of NMC), however, experienced difficulty with both the barotropic and baroclinic forecast models when the geostrophic approximation was used to calculate initial wind (Cressman and Hubert, 1957). Although these models are based on quasi-geostrophic and thermal wind assumptions, this initial wind field contains information which is inconsistent with the governing equations, i.e., the field contains noise. This was first pointed out by Shuman (1957). The importance of consistency between the initial map and the equations was further emphasized by Sasaki (1958). Especially significant in the latter investigation was the simultaneous calculation of wind, geopotential, and temperature fields satisfying geostrophic and thermal wind conditions.

Improvement in JNWP forecasts resulted when initial winds were obtained from the "balance equation." Since this equation is a generalization of the geostrophic relation, knowledge of the geopotential field is sufficient to determine the wind. Charney (1955) derived this equation by taking the divergence of the horizontal equation of motion in the primitive set. The development assumes that the horizontal divergence and its tendency vanish. The unwanted high frequency gravity-inertia waves are characterized by relatively large divergence. Consequently, it is conceivable that the initial field determined from the balance equation eliminates the noise and passes the meteorologically significant information.

However, both Sasaki (1958) and Phillips (1960) showed that the balance condition can admit unwanted noise and filter important low fre-

quency information. When the balance equation is solved by using either a subjectively analyzed geopotential or a geopotential field obtained by a geostrophic analysis, the balanced wind is not noise-free. Sasaki's (1958) variational objective analysis modifies both the wind and geopotential in such a way that the balance condition is satisfied.

Phillips (1960) showed that some initial divergence is necessary to suppress the gravity-inertia waves when forecasting with the primitive equations. The amount of divergence is that implied by the quasi-geostrophic system of forecasting. In principle, the balance condition suppresses some necessary low frequency information along with the unwanted high frequency noise. Accordingly, a plan is underway at NMC to incorporate divergence into the initial wind map (Stackpole, 1968). This is accomplished by using the 12 hr forecast from previous initial conditions. The divergent part of this forecasted wind field is extracted and added to the non-divergent wind obtained from the balance equation.

Until recently, objective analysis of initial fields has been based on diagnostic relations such as the geostrophic relation and balance equation. Within the past year, two investigations (Miyakoda and Moyer, 1968; Sasaki, 1969) have directly incorporated the governing prognostic equations into the initialization process. Thus, consistency between the initial map and the time dependent governing equations is accomplished.

Miyakoda and Moyer (1968) have essentially developed a new technique to solve the balance equation. With their method, the physical processes of friction or heating can be handled whereas this is impossible

with the conventional solution to the balance equation.

Sasaki's (1969) approach is an extension of his previous study (1958) based upon the variational principle. Whereas the earlier development was limited to diagnostic constraints such as hydrostatic and geostrophic balance, the present method includes the effects of time variations appearing in the prognostic equations. A primary advantage of this technique is its ability to produce dynamically consistent initial fields for all the variables in the atmospheric model, not just wind. Additionally, there is the capability of producing dynamically sound initial values in the areas or layers of lacking observation.

Sasaki's method is capable of handling the small space and time scales required in the planetary boundary layer model. This model is designed to account for the physical processes within the lowest several kilometers of so-called local weather systems which are characterized by horizontal dimensions of  $10^2 - 10^3$  km and a life span the order of 10 hr. Since the time scale associated with these events is relatively short compared to the quasi-geostrophic motions, the initial fields play an increasingly important role in the prediction process. Also, the initial distribution of moisture, temperature, and pressure must be given the same degree of attention that the wind field has previously received.

In view of these facts, the method of Sasaki is used for this investigation. A set of analysis equations is derived which incorporates observations, governing thermo-hydrodynamic equations, and diagnostic dynamical constraints. To demonstrate the technique of initialization, a case study characterizing severe weather development is undertaken.

## CHAPTER II

### METHOD OF OBJECTIVE ANALYSIS

The method of the dynamical objective analysis described in this chapter is based on Sasaki's recent unpublished note\* on the objective analysis of the planetary boundary layer. The variational form is given as the following:

$$\begin{aligned}
 \delta \sum_{ijk} \{ & \alpha_1 (\theta_1 - \theta_0)^2 + \tilde{\alpha} (\theta_0 - \tilde{\theta})^2 + \nu_1 (\varphi_1 - \varphi_0)^2 \\
 & + \tilde{\nu} (\varphi_0 - \tilde{\varphi})^2 + \gamma_1 (u_1 - u_0)^2 + \gamma_1 (v_1 - v_0)^2 \\
 & + \tilde{\gamma} (u_0 - \tilde{u})^2 + \tilde{\gamma} (v_0 - \tilde{v})^2 + \chi_1 (q_1 - q_0)^2 \\
 & + \tilde{\chi} (q_0 - \tilde{q})^2 + \epsilon (\nabla_{\sigma} \varphi_0 - \mu \theta_0)^2 + \eta (\nabla_x u_0 + \nabla_y v_0)^2 \} \\
 & = 0
 \end{aligned} \tag{1}$$

where  $\delta$  represents the variational operator. The indices  $i$ ,  $j$ , and  $k$  are integers assigned to each grid point of the three dimensional lattice used, and  $\sum_{ijk}$  represents the total sum of the quantities over the entire set of lattice points. The meteorological variables are symbolized according to the convention adopted in Appendix A. Each variable represents a non-dimensional perturbation upon the basic state as explained in this same Appendix.

---

\*Personal communication

Expression (1) contains information on each meteorological variable at two time levels, initial and forecast. Observations of the variables at initial time are designated by  $\tilde{\Phi}$ , where  $\Phi$  represents an arbitrary variable which is a function of  $i$ ,  $j$ , and  $k$ . The forecasted values are denoted by  $\Phi_1$ , and the "true" value at analysis time by  $\Phi_0$ . Weights  $\alpha_1$ ,  $\tilde{\alpha}$ , etc., ( $>0$ ), again functions of  $i$ ,  $j$ , and  $k$ , are arbitrarily chosen under the condition that  $\alpha_1 = 0$  at a particular grid point if  $\theta_1$  and/or  $\theta_0$  are missing at this point. Similarly,  $\tilde{\alpha} = 0$  if  $\tilde{\theta}$  and/or  $\theta_0$  are missing. The above argument holds for the remaining weights.

The time increment between the forecast and initial time is inherently related to the time scale incorporated into the governing dynamical equations, (A - 48) through (A - 55). The governing set of equations is designed to describe the propagation of low frequency internal waves whose scale is the order of 10 hours. The time increment should also be consistent with the difference scheme used to make an extended forecast. That is, the time step is limited by computational stability and truncation error requirements contained in the finite difference analog used to forecast. In view of the above considerations, the forecasted time level depicted in (1) is 15 minutes after initial time.

The last two terms in (1) are called diagnostic dynamical constraints. For this investigation, the constraints used are horizontal non-divergence and hydrostatic balance. The use of the word constraint does not imply that the initial fields are to be in hydrostatic balance and non-divergent. Instead, the adjusted fields satisfy these constraints

in accord with the relative weight on the multipliers  $\epsilon$  and  $\eta$ .

A myriad collection of possible initial fields can be obtained by varying the relative magnitudes of the set of multipliers. However, factors such as reliability of observations and density of observations generally control the choices. For example, in data sparse regions, weighting must favor the governing dynamic equations. Consequently, the ratios  $\alpha_1/\tilde{\alpha}$ ,  $\gamma_1/\tilde{\gamma}$ , etc., should be large for regions where observations are suspect or infinite in regions of no data. Similarly, if pressure observations are "better" than wind observations, the ratio  $\tilde{v}/\tilde{\gamma}$  should be greater than 1.

A necessary condition for obtaining a stationary value for a functional is the vanishing of its first variation. This is precisely the condition expressed by (1). To find an extremum generally requires further conditions on the second variation. Nevertheless, investigation of the second variation for this problem is superfluous. That is, the functional to be minimized is composed of purely positive terms; consequently, the solution obtained by the requirement of stationarity automatically yields a solution which minimizes the integral (see Lanczos, 1966).

Before performing the manipulations associated with variational calculus, several rules are reviewed:

- i. Variation and differentiation are permutable processes, thus

$$\delta \nabla_{\mathbf{x}} \varphi = \nabla_{\mathbf{x}} \delta \varphi$$

- ii. Variation and integration are permutable processes, thus

$$\delta \sum_{ijk} ( ) = \sum_{ijk} \delta ( )$$

Another property that results from the special choice of spatial difference scheme is

$$\sum_{ijk} \psi \nabla_x \varphi = - \sum_{ijk} \varphi \nabla_x \psi$$

iii.

$$\sum_{ijk} \psi \nabla_x (\xi \nabla_x \varphi) = \sum_{ijk} \varphi \nabla_x (\xi \nabla_x \psi)$$

where the operators  $\nabla_y$  and  $\nabla_\sigma$  could also be used.

Operating on (1) with the use of the foregoing properties, we get

$$\sum_{\text{interior}} U \delta u_0 + V \delta v_0 + \Theta \delta \theta_0 + Q \delta q_0 = 0 \quad (2)$$

where

$$U = \left\{ \begin{aligned} & \gamma_1 \Delta t \nabla_x u_0 (u_1 - u_0) + \gamma_1 \Delta t \nabla_y v_0 (u_1 - u_0) \\ & - \gamma_1 \Delta t (u_1 - u_0) \nabla_x u_0 + \gamma_1 \Delta t \frac{\Lambda_M}{Ro} \nabla_\sigma^2 (u_1 - u_0) \\ & - \frac{\gamma_1 \Delta t}{Ro} (v_1 - v_0) - \gamma_1 \Delta t (v_1 - v_0) \nabla_x v_0 \\ & + \tilde{\gamma} (u_0 - \tilde{u}) - \eta \nabla_x (\nabla_x u_0 + \nabla_y v_0) \\ & - \chi_1 (q_1 - q_0) \nabla_x q_0 - (\theta_1 - \theta_0) \Delta t (\alpha_1 + v_1 \beta^2) \nabla_x \theta_0 \\ & + \gamma_1 \Delta t \nabla_\sigma (u_1 - u_0) w_0^* \end{aligned} \right. \quad (3)$$

$$\begin{aligned}
 v = & \left\{ \begin{aligned}
 & \gamma_1 \Delta t \nabla_x u_0 (v_1 - v_0) + \gamma_1 \Delta t \nabla_y v_0 (v_1 - v_0) \\
 & - \gamma_1 \Delta t (v_1 - v_0) \nabla_y v_0 + \gamma_1 \Delta t \frac{\Lambda_M}{Ro} \nabla_\sigma^2 (v_1 - v_0) \\
 & + \gamma_1 (u_1 - u_0) \frac{\Delta t}{Ro} - \gamma_1 \Delta t (u_1 - u_0) \nabla_y u_0 \\
 & + \tilde{\gamma} (v_0 - \tilde{v}) - \eta \nabla_y (\nabla_x u_0 + \nabla_y v_0) \\
 & - \chi_1 (q_1 - q_0) \nabla_y q_0 + \gamma_1 \Delta t \nabla_\sigma w_0^* (v_1 - v_0) \\
 & - (\theta_1 - \theta_0) \Delta t (\alpha_1 + \nu_1 \beta^2) \nabla_y \theta_0
 \end{aligned} \right. \quad (4)
 \end{aligned}$$

$$\begin{aligned}
 \theta = & \left\{ \begin{aligned}
 & (\alpha_1 + \nu_1 \beta^2) \Delta t \cdot [ \nabla_x u_0 (\theta_1 - \theta_0) + \nabla_y v_0 (\theta_1 - \theta_0) ] \\
 & + (\alpha_1 + \nu_1 \beta^2) \Delta t \cdot [ \nabla_\sigma w_0^* (\theta_1 - \theta_0) + \Lambda_H \nabla_\sigma^2 (\theta_1 - \theta_0) ] \\
 & + \tilde{\alpha} (\theta_0 - \tilde{\theta}) + \tilde{\nu} \beta (\varphi_0 - \tilde{\varphi}) \\
 & + \epsilon (\mu^2 \theta_0 + \mu \beta \nabla_\sigma \theta_0 - \mu \nabla_\sigma \varphi_0 - \beta \nabla_\sigma^2 \varphi_0) \\
 & + \frac{\gamma_1 \Delta t}{Ro} \beta \nabla_x (u_1 - u_0) + \left( \frac{\gamma_1 \Delta t}{Ro} \mu \nabla_x h \right) (u_1 - u_0) \\
 & + \frac{\gamma_1 \Delta t}{Ro} \beta \nabla_y (v_1 - v_0) + \left( \frac{\gamma_1 \Delta t}{Ro} \mu \nabla_y h \right) (v_1 - v_0)
 \end{aligned} \right. \quad (5)
 \end{aligned}$$

$$Q = \begin{cases} \tilde{\chi}(q_0 - \tilde{q}) + \chi_1 \Delta t \nabla_{\sigma} w_0^* (q_1 - q_0) \\ + \chi_1 \Delta t \nabla_x u_0 (q_1 - q_0) + \chi_1 \Delta t \nabla_y v_0 (q_1 - q_0) \end{cases} \quad (6)$$

It is necessary to use the governing thermo-hydrodynamic equations, (A - 62) through (A - 67), to obtain the form shown. Also, the eddy coefficients of heat and momentum have been assumed constant and equal to their scale values.

The variations of  $\varphi_0$  and  $w_0^*$  do not appear in (2) because they are not independent of  $u_0$ ,  $v_0$ ,  $\theta_0$ , and  $q_0$ . These latter four variables form the basis of the function space. The variation of each member of the basic set is arbitrary at each grid point and consequently,

$$U(u_0, v_0, \dots; \tilde{u}, \tilde{v}, \dots; \alpha_1, \gamma_1, \dots) = 0 \quad (7)$$

$$V(u_0, v_0, \dots; \tilde{u}, \tilde{v}, \dots; \alpha_1, \gamma_1, \dots) = 0 \quad (8)$$

$$\Theta(u_0, v_0, \dots; \tilde{u}, \tilde{v}, \dots; \alpha_1, \gamma_1, \dots) = 0 \quad (9)$$

$$Q(u_0, v_0, \dots; \tilde{u}, \tilde{v}, \dots; \alpha_1, \gamma_1, \dots) = 0 \quad (10)$$

The relations (7) - (10) hold at each mesh point interior to the bounding region. The equation set (7) - (10) is referred to classically as the Euler-Lagrange equations. However, these equations will be called the analysis equations in accord with the nomenclature of Sasaki (1968b).

#### Boundary Conditions

There is more than one set of boundary conditions which will satisfy

(1). A full scale study of the so-called natural boundary conditions con-

sistent with (1) should be undertaken (see Lanzcos, 1966). However to obtain some immediate practical results, the detailed investigation is omitted. The simplest type boundary conditions are formulated at the lateral boundaries and the top, viz., Dirichlet conditions. These conditions allow no variation in the dependent variables, i.e., a fixed condition. At the top of the planetary boundary layer, the wind, moisture, and temperature fields are given by the large scale flow features as obtained from the NMC objective analysis (Cressman, 1959). In a similar fashion, the fields on the lateral boundaries are fixed by taking information from the nearest radiosonde station.

Boundary conditions at the lower boundary are formulated to account for heat and momentum transfer. The development follows Kasahara and Washington (1967), i.e.,

$$\nabla_{\sigma} u_0 = A C_D \left| \vec{v}_H \right| u_0 \quad (11)$$

$$\nabla_{\sigma} v_0 = A C_D \left| \vec{v}_H \right| v_0 \quad (12)$$

$$\nabla_{\sigma} \theta_0 = B C_D \left| \vec{v}_H \right| \theta_0 \quad (13)$$

where

$$A = \frac{v_0 z_0}{K_{MO}} = 10^4$$

$$B = \frac{v_0 z_0}{K_{HO}} = 10^4$$

$$\left| \vec{v}_H \right| = \sqrt{u_0^2 + v_0^2}$$

$\tau$  : surface stress

$$C_D = \tau \rho_0^{-1} |\vec{v}_H|^{-2} \quad (\text{drag coefficient})$$

The drag coefficients calculated at NMC (Cressman, 1960) are used for this investigation. The numerical values of the coefficients essentially discriminate between the drag over flat land or over ocean and the form drag of the large scale relief of the earth's surface. Contours of  $C_D$  are shown in Fig. 2.

### Numerical Method of Solution

The solution of the system of analysis equations (7) - (10) with the accompanying boundary conditions is obtained through use of the Richardson method (Richardson, 1911). This relaxation method is designed for application to the difference form of elliptic partial differential equations and the associated boundary conditions. The analysis equations are fourth order, and formal proof of their elliptic nature is a formidable problem. Sasaki (1969) has demonstrated the applicability of relaxation methods to analysis equations consisting of advection and diffusion constraints.

The Richardson method is iterative and involves successively applied local corrections to improve an approximate solution. Let  $u_0^{(1)}$ ,  $v_0^{(1)}$ ,  $\theta_0^{(1)}$ , and  $q_0^{(1)}$  be a first (guessed) approximation to the initial fields at a particular grid point interior to the specified domain. Now each of the succeeding approximations,  $u_0^{(2)}$ ,  $v_0^{(2)}$ ,  $\theta_0^{(2)}$ ,  $q_0^{(2)}$ , etc., is calculated on the basis of its immediate predecessor. In order to develop the iteration procedure, the analysis equations are written in terms of the approximate solution at the pth stage:

$$U(u_0^{(p)}, v_0^{(p)}, \dots; \tilde{u}, \tilde{v}, \dots; \alpha_1, \gamma_1, \dots) = R_u^{(p)} \quad (14)$$

$$V(u_0^{(p)}, v_0^{(p)}, \dots; \tilde{u}, \tilde{v}, \dots; \alpha_1, \gamma_1, \dots) = R_v^{(p)} \quad (15)$$

$$\Theta(u_0^{(p)}, v_0^{(p)}, \dots; \tilde{u}, \tilde{v}, \dots; \alpha_1, \gamma_1, \dots) = R_\theta^{(p)} \quad (16)$$

$$Q(u_0^{(p)}, v_0^{(p)}, \dots; \tilde{u}, \tilde{v}, \dots; \alpha_1, \gamma_1, \dots) = R_q^{(p)} \quad (17)$$

where  $R_u^{(p)}$ ,  $R_v^{(p)}$ ,  $R_\theta^{(p)}$  and  $R_q^{(p)}$  represent the residues at the  $p$ th iteration. The corrections at the  $(p+1)$ st stage are calculated so as to minimize  $R_u^{(p)}$ ,  $R_v^{(p)}$ ,  $R_\theta^{(p)}$  and  $R_q^{(p)}$ . Reduction of the residue is achieved by the following iteration formulas:

$$u_0^{(p+1)} = u_0^{(p)} + \alpha_u^{(p)} R_u^{(p)} \quad (18)$$

$$v_0^{(p+1)} = v_0^{(p)} + \alpha_v^{(p)} R_v^{(p)} \quad (19)$$

$$\theta_0^{(p+1)} = \theta_0^{(p)} + \alpha_\theta^{(p)} R_\theta^{(p)} \quad (20)$$

$$q_0^{(p+1)} = q_0^{(p)} + \alpha_q^{(p)} R_q^{(p)} \quad (21)$$

where

$$\frac{1}{\alpha_u^{(p)}} = \frac{1}{\alpha_v^{(p)}} = \left\{ \begin{array}{l} \tilde{\gamma} + \frac{2\pi}{(2\Delta s)^2} + 2\gamma_1 \left( \frac{\Delta t}{2\Delta s} \right)^2 ([\bar{u}_0^{(p)}]^2 + [\bar{v}_0^{(p)}]^2) \\ + \gamma_1 \left( \frac{\Delta t}{Ro} \right)^2 \left( 1 + 6 \left[ \frac{\Lambda_M}{(2\Delta\sigma)^2} \right]^2 \right) \end{array} \right.$$

$$-\frac{1}{\alpha_{\theta}(p)} = \left\{ \begin{aligned} & (\alpha_1 + \nu_1 \beta^2) (2[\frac{\Delta t}{2\Delta s}]^2 \cdot [(\bar{u}_0(p))^2 + (\bar{v}_0(p))^2] + 6[\frac{\Lambda_H}{(2\Delta\sigma)^2}]^2) \\ & + \tilde{\alpha} + \beta\tilde{\nu} + \epsilon (\mu^2 + 2[\frac{\beta}{2\Delta\sigma}]^2) \\ & + \gamma_1 (\frac{\Delta t}{Ro})^2 \cdot ([\frac{\beta}{\Delta s}]^2 + [\mu\nabla_x h]^2 + [\mu\nabla_y h]^2) \end{aligned} \right.$$

$$-\frac{1}{\alpha_q(p)} = \tilde{\chi} + 2\chi_1 \cdot (\frac{\Delta t}{2\Delta s})^2 \cdot ([\bar{u}_0(p)]^2 + [\bar{v}_0(p)]^2)$$

and  $\Delta s$ ,  $\Delta\sigma$ , and  $\Delta t$  are the horizontal space, vertical space, and time increments, respectively. The local average values of  $u_0(p)$  and  $v_0(p)$  are denoted by  $\bar{u}_0(p)$  and  $\bar{v}_0(p)$ . The fields of  $\varphi_0$  and  $w_0$  are determined at each stage through the gas law and mass conservation, respectively. Examination of the convergence of the iterative scheme is discussed in Appendix B.

## CHAPTER III

### APPLICATION TO A CASE OF SQUALL LINE FORMATION

The method of analysis is applied to severe weather occurrences in the Midwest during the time period 00 GMT June 10, 1968, to 06 GMT June 10, 1968. A horizontal mesh size of 190 km and a vertical grid length of 200 m are used. The horizontal grid length is chosen exactly half the NMC grid length and the lattice of points overlaps the operational NMC grid. The vertical spacing is displayed in Fig. 3. The three-dimensional lattice covers an area whose dimensions are approximately 2000 km x 2000 km x 2 km.

Two essentially different sources of meteorological data are used for the analysis. First, wind and moisture information are collected from the radiosonde stations located within the network (see Fig. 4). Pressure and temperature information are obtained from the NMC objective analysis. The pressure and temperature data could be extracted from the radiosonde records for a somewhat more consistent set of data. However, the hybrid collection of information helps to reveal the versatility of the variational method. The degree of confidence in each data set is controlled by appropriate choice of magnitudes of the weights.

The boundary conditions discussed in Chapter II require the specification of the meteorological fields on the bounding surfaces. At all boundaries, the pressure and temperature fields are found by interpolation from the NMC objective analysis. Since this analysis is

only available at the standard levels (1000 mb, 850 mb, 700 mb were used in this study) and at the NMC grid points, both vertical and horizontal interpolations are necessary.

First, the hydrostatic assumption is used to obtain pressure and temperature on the bounding  $\sigma$ -surfaces. The perturbation fields are then extracted according to the formulas in Appendix A. Perturbations of temperature and pressure at the grid points intermediate to the NMC points are then found by simple averaging.

Wind and moisture fields at the lower and lateral boundaries are determined from the radiosonde observations. The wind and specific humidity profiles at the nearest radiosonde site are assumed valid at the particular boundary point. Since there are only 35 sites within the model network, there is certainly error in this specification. Ideally, information from the dense network of stations reporting meteorological variables at the surface (WBAN reports) should be used to formulate the lower boundary condition. However, in an effort to immediately demonstrate the feasibility of this variational technique, the lower boundary condition was formulated in terms of the processed data from the radiosonde network.

The wind field at the upper boundary is designed to reflect the large-scale flow features in the free atmosphere. Consequently, the wind field at this level was derived from the 850 mb and 700 mb objective wind analyses produced by NMC.

Points interior to the bounding planes are classified into two categories: (1) points which possess wind and moisture observations, (2) points which do not possess wind and moisture observations. Observations of wind

and specific humidity at a given radiosonde station are assumed valid at the nearest interior grid point. Consequently, approximately 20% of the interior grid points have wind and specific humidity observations. All points have temperature and pressure information. These data come from the NMC analysis. Although this does not constitute a source of raw data, a certain weight can be attached to this information source through appropriate specification of the weights.

### Weights

A decision must now be made to determine the relative weights of the Lagrange multipliers. From the discussion in the previous section, there should be two distinct sets of multipliers, i.e., one for each category of interior points. The two sets of multipliers are designated as follows: (1) set A, interior points with wind and moisture observations, (2) set B, interior points with no wind and moisture observations.

	$\epsilon = 1.0 \times 10^0$	
set A:	$\tilde{\chi} = 5.0 \times 10^{-1}$	$\chi_1 = 5.0 \times 10^{-1}$
	$\tilde{\gamma} = 5.0 \times 10^{-1}$	$\gamma_1 = 5.0 \times 10^{-1}$
	$\tilde{\alpha} = 1.0 \times 10^{-1}$	$\alpha_1 = 1.0 \times 10^0$
	$\tilde{\nu} = 1.0 \times 10^{-1}$	$\nu_1 = 1.0 \times 10^0$
	$\eta = 1.0 \times 10^{-3}$	

$$\begin{array}{rcl}
 \epsilon & = & 1.0 \times 10^0 \\
 \tilde{\chi} & = & 0 \\
 \tilde{\gamma} & = & 0 \\
 \text{set B: } \tilde{\alpha} & = & 1.0 \times 10^{-1} \\
 \tilde{\nu} & = & 1.0 \times 10^{-1} \\
 \tilde{\eta} & = & 1.0 \times 10^{-3} \\
 \chi_1 & = & 5.0 \times 10^{-1} \\
 \gamma_1 & = & 5.0 \times 10^{-1} \\
 \alpha_1 & = & 1.0 \times 10^0 \\
 \nu_1 & = & 1.0 \times 10^0
 \end{array}$$

The only difference between the two sets is the weight on  $\tilde{\chi}$  and  $\tilde{\gamma}$ , the multipliers related to observed specific humidity and wind, respectively.

To a certain extent, these multipliers are chosen in a purely arbitrary manner. However, some consideration is given to the mathematical restrictions inherent in the iterative method of solution. The formal treatment of this aspect of the problem is discussed in Appendix B. As suggested in that Appendix, the myriad possibilities for sets of multipliers requires an exhaustive study. The present investigation only attempts to find a satisfactory set which produces initial fields suitable for dynamic forecasting in the boundary layer.\*

A brief outline of the method used for determining set A will be given. Assuming all multipliers zero except  $\alpha_1$ ,  $\nu_1$ ,  $\gamma_1$ , the eigenvalues of the amplification matrix are computed. The QR-method of Francis (1961a; 1961b) is used

---

\*Sasaki's objective analysis method used in this study is sensitive to the convergence of iterative solution. After the first method, Sasaki developed a second method which is not sensitive to the convergence and has used it in mesometeorological analyses. (Personal communication)

to find the eigenvalues of this matrix. The results indicated that the iterative scheme is convergent when the ratios  $\gamma_1/\alpha_1$  and  $\gamma_1/\nu_1$  are less than 1. At this point, the weights on  $\tilde{\alpha}$  and  $\tilde{\nu}$  are chosen arbitrarily as 1/10 and, in conformity with the above results,  $\gamma_1/\alpha_1$  and  $\gamma_1/\nu_1$  are chosen to be 5/10. The multipliers on the diagnostic dynamical constraints,  $\epsilon$  and  $\eta$ , are then examined. A ratio of  $\epsilon/\eta$  the order of  $10^3$  gave the smallest spectral radius when used in conjunction with the other fixed multipliers. A range of possible  $\tilde{\gamma}$  values is then examined and a plot of the spectral radius as a function of  $\tilde{\gamma}$  is shown in Fig. 5. Based on this graph, the weight on  $\tilde{\gamma}$  is chosen as 5/10 implying equal weight on observation and forecast, i.e.,  $\tilde{\gamma} = \gamma_1 = 5/10$ . Weighting for the specific humidity is chosen in conformity with the weighting for the winds.

#### The Initial Fields

The iterative solution for initial fields of  $u$ ,  $v$ ,  $w^*$ ,  $\varphi$ ,  $q$ , and  $\theta$  are found by use of Richardson's method. The rate of convergence is measured by a cumulative residual over the interior points. Standard deviations for the four basic fields are defined as follows:

$$D_u = \sqrt{\frac{\sum_{ijk} R_u^2}{N}} \quad (22)$$

$$D_v = \sqrt{\frac{\sum_{ijk} R_v^2}{N}} \quad (23)$$

$$D_\theta = \sqrt{\frac{\sum_{ijk} R_\theta^2}{N}} \quad (24)$$

$$D_q = \sqrt{\frac{\sum_{ijk} R_q^2}{N}} \quad (25)$$

where  $N$  is the number of interior points and the summation is taken over the interior points. Graphs of the convergence rates are displayed in Fig. 6.

The fields show a rapid rate of convergence between 1 and 5 iterations. However, there is an obvious increase in the standard deviation which appears first in the  $q$ -field at the 6th iteration. No reference to this type of instability has been found in applied mathematical or physical science literature. This instability may have stemmed from the linear development of the iteration formulae. That is, the iteration schemes (18) - (21) were derived by linearizing the analysis equations. These same iteration schemes were then applied to the non-linear form of analysis equations.

The adjustment of the meteorological fields after eight iterations is used to represent the initial state. The standard deviations for the wind components were reduced from an initial value of  $10^{-2}$  to  $1.1 \times 10^{-3}$  within eight iterations. The  $q$ -field fell from  $8 \times 10^{-4}$  to  $10^{-4}$ . Although the  $\theta$ -field showed only a slight reduction, the initial adjustment was strong as evidenced by the peak at the second iteration. At this stage of the iterative process the  $u$ ,  $v$ , and  $q$ -fields have just started to diverge and the  $\theta$ -field is yet unaffected. Until the nature of this iterative instability is clarified, a subjective decision is necessary to choose the iterative stage that best represents the adjusted meteorological fields.

In addition to providing the necessary information for integrating the governing thermo-hydrodynamical equations, the initial fields have value as a

diagnostic tool. This is demonstrated by calculating  $wq$ , the product of the vertical velocity (not  $w^*$ ) and the specific humidity, at  $t = 0$ . Sasaki et al. (1967) introduced this objective severe storm index and illustrated its usefulness for delineating areas of severe weather occurrence. The distribution of this parameter at level 5 and at 00 GMT June 10, 1968, is displayed in Fig. 7a. The surface observations of meteorological activity at this time are shown beside the distribution of  $wq$ . This index is designed to depict areas where there is a large vertical flux of moisture out of the boundary layer. Also, since  $q \geq 0$ , upward and downward transport of moisture is immediately evident from the sign of the index. The thunderstorm activity and convective motion essentially occur in the region of positive  $wq$  at 00 GMT June 10. It must be mentioned that verification in Nebraska, northern Iowa, and southern Wisconsin, was not possible because of inaccessible teletype reports. This unrepresented area, however, accounts for less than 10% of the grid considered.

#### Short Range Forecast

Using 00 GMT June 10, 1968, as the initial ( $t = 0$ ) time, a 6 hr forecast is made using the model described in Appendix A. The initial fields are derived by the techniques developed in the previous section. In order to extend the forecast, coupling with a mid-tropospheric model would be necessary. The interaction between the planetary boundary layer and the free atmosphere could then be handled through the upper level boundary condition. The present investigation, however, assumes that the fields are fixed at this top level for the duration of the forecast.

Equations (A - 62) through (A - 67) are used for the first four time steps with  $\Delta t = 7.5$  min. Following this initial integration, a centered time step is used with  $\Delta t = 15$  min. This latter time step is chosen in accord with the von Neumann condition for computational stability (Richtmyer, 1963). The boundary conditions are consistent with those used for initialization as discussed in Chapter II.

Attention is centered on the forecast of objective indices for predicting severe storm occurrences. There are many empirical rules and indices that have been used operationally (see Miller, 1967). Notable success has been achieved by Reap and Alaka (1969). They have introduced an index which incorporates the vertical profiles of equivalent potential temperature and net 6 hr vertical displacements of parcels. The index  $wq$ , mentioned earlier, is especially easy to calculate from the output of the boundary layer model. Consequently, this index is used to demonstrate the forecasting capabilities of the model. In addition, an examination of the humidity field and its associated gradient is made.

ESSA-5 satellite photos depicting the meteorological conditions in the Midwest on June 9 and June 10 are shown in Fig. 13 and Fig. 14, respectively. The time of each photograph is late afternoon on each of the two days. Although the photos cannot be used to verify the initialization and forecast, some general large scale flow features in the free atmosphere along with imbedded mesoscale activity are evident.

The initial and forecast fields of  $wq$  and  $q$ , at the mid-level of the model, are contoured in Figs. 7 - 12. The intensification of the index is

evident over the 6 hr forecast period. Especially satisfying is the position of the maximum on the 6 hr forecast in relation to the severe weather observations from the surface recording stations. The spread of thunderstorm activity toward the southeast between  $t = 3$  hr and  $t = 6$  hr is also indicated by the  $wq$  distributions. The moisture forecast indicates an increase in the specific humidity gradient along the so-called dry front which is oriented from southwest to northeast and extends from eastern New Mexico into Nebraska. The forecast of this gradient appears to be related to the observed severe weather. However, the areal resolution of  $wq$  is noticeably better. Reap and Alaka (1969) found a similar relation between the 1000 mb dew point gradient and their index which incorporated vertical velocity and equivalent potential temperature.

## CHAPTER IV

### CONCLUSIONS AND REMARKS

The method of dynamic objective analysis using the variational principle is applied to atmospheric systems of horizontal space scale  $10^2 - 10^3$  km and time scale the order of 10 hr. This technique incorporates the governing thermo-hydrodynamical equations, as well as the observations, into the initialization process. Incorporation of the governing equations does not imply a marching process in time; instead, an iterative process is developed which is centered around  $t = 0$ , initial time. The analysis equations used in the iterative process are a system of elliptic difference equations which are solved using the Richardson relaxation method.

Dynamically sound initial values can be obtained in areas or layers where observations are missing. This is accomplished by permitting the governing dynamics to generate the initial values. The relative weight on dynamics and observations is controlled through the specification of the Lagrange multipliers. These multipliers are arbitrarily chosen within the framework of the analytic theory. However, the numerical method of solution does impose some constraints on the relative magnitudes of the multipliers. These restrictions are necessary to obtain iteratively convergent solutions to the analysis equations.

The technique is demonstrated by application to a case of severe weather development in the Midwest. Data from the radiosonde network and the NMC objective analysis are used to generate the initial fields. The 8 layer forecast model encompasses a volume of approximately 2000 km x 2000 km x 2 km and incorporates a horizontal grid interval of 190 km and vertical spacing of 200 m.

The usefulness of the index  $wq$  in delineating areas of severe storm activity is demonstrated. Also, the ability of the model to predict intensification of storm activity is shown in the 3 and 6 hr forecasts. Although the forecast position of the dry front appears closely related to the occurrence of severe weather, the areal resolution is incomplete.

Since the governing analysis equations are elliptic, i.e., determined by boundary values, the objective analysis for a smaller grid interval seems plausible in theory. Also, the use of surface reports (hourly observations) will give a more reliable lower boundary condition.

The coupling of the boundary layer model with a model for the mid-troposphere is necessary to extend the forecast period. The model must eventually include the diabatic effects of radiation and latent heat. The inclusion of these processes, however, has lower priority than the problem of coordinating the forecasts of the boundary layer and free atmosphere.

## REFERENCES

- Arnason, G., 1958: A convergent method for solving the balance equation. J. Meteorology, 15, 220-225.
- Baddley, H., 1968: Investigation of Wind and Temperature Profiles in the Planetary Boundary Layer. Master's Thesis, University of Oklahoma, 54 pp.
- Charney, J.G., 1955: The use of the primitive equations of motion in numerical prediction. Tellus, 7, 22-26.
- Cressman, G.P., and W.E. Hubert, 1957: A study of numerical forecasting errors. Monthly Weather Review, 85, 235-242.
- Cressman, G.P., 1957: An Objective Analysis Study. Tech. Memo. No. 12, Joint Numerical Weather Prediction Unit, Suitland, Maryland, 12 pp.
- \_\_\_\_\_, 1960: Improved terrain effects in barotropic forecasts. Monthly Weather Review, 88, 327-342.
- Francis, J.F.G., 1961a: The QR transformation: Part I. Computer Journal, 4, 265-271.
- \_\_\_\_\_, 1961b: The QR transformation: Part II. Computer Journal, 4, 332-345.
- Frankel, S.P., 1950: Convergence rates of iterative treatments of partial differential equations. Math. Tables and Other Aids to Computation, 4, 65-75.
- Hinkelmann, K., 1951: Der mechanismus des meteorologischen Lärmes. Tellus, 3, 285-296.
- Kasahara, A., and W.M. Washington, 1967: NCAR global general circulation model of the atmosphere. Monthly Weather Review, 95, 389-402.
- Lanczos, C., 1966: The Variational Principles of Mechanics. University of Toronto Press, Toronto, Canada, Math. Expositions No. 4, 375 pp.
- List, Robert J., 1966: Smithsonian Meteorological Tables, Vol. 115, Smithsonian Miscellaneous Collections, Washington, D.C., 527 pp.

- Miller, R.C., 1967: Notes on Analysis and Severe Storm Forecasting Procedures of the Military Weather Warning Center. Air Weather Service Tech. Rept., No. 200, 125 pp.
- Miyakoda, K., and R.W. Moyer, 1968: A method of initialization for dynamic weather forecasting. Tellus, 20, 115-127.
- Monin, A.S., and A.M. Obukhov, 1958: Slight fluctuations of the atmosphere and adoption of meteorological fields. Izv., Geophy. Ser., 4, 1360-1373.
- Ogura, Y., 1963: A review of numerical modeling research on small scale convection in the atmosphere. Meteor. Monographs, Vol. 5, No. 27, pp. 65-76.
- Payn, F., 1967: Velocity Profiles in the Boundary Layer up to 500 Meters. Master's Thesis. University of Oklahoma, 59 pp.
- Phillips, N.A., 1960: On the problem of initial data for the primitive equations. Tellus, 12, 121-126.
- Reap, R.M., and M.A. Alaka, 1969: An Objective Quasi-Lagrangian Index for Predicting Convective Weather Outbreaks. Proceedings of Sixth Conference on Severe Local Storms, Chicago, Illinois. (Unpublished manuscript)
- Richardson, L.F., 1911: The approximate arithmetical solution by finite differences of physical problems involving differential equations, with an application to the stresses in a masonry dam. Phil. Trans. Roy. Soc. London, Ser. A, 210, 307-357.
- Richtmyer, R.D., 1963: A Survey of Difference Methods for Non-Steady Fluid Dynamics. NCAR Tech. Notes 63-2, National Center for Atmospheric Research, Boulder, Colorado, 25 pp.
- Richtmyer, R.D., and K.W. Morton, 1967: Difference Methods for Initial Value Problems. Interscience, New York, 405 pp.
- Sasaki, Y., 1958: An objective analysis based on the variational method. J. Meteor. Soc. Japan, 36, 77-88.
- Sasaki, Y., J.M. Lewis, T.S. Chen, L. French, and J. Harmon, 1967: Dynamical Forecasting of Severe Local Storms. University of Oklahoma Research Institute Report, December, 1967, 20 pp.
- Sasaki, Y., 1968a: Numerical Variational Method of Analysis and Prediction. Proceedings WMO/IUGG Symposium on Numerical Weather Prediction, Tokyo, Japan, November, 1968. (Unpublished manuscript)

- \_\_\_\_\_, 1968b: Numerical Variational Method of Objective Analysis: Principle of Initialization. University of Oklahoma Research Institute Rept. No. 10, 21 pp.
- \_\_\_\_\_, 1969: Proposed inclusion of time variation terms, observational and theoretical, in numerical variational objective analysis. (Accepted for publication in the April, 1969, issue of J. Meteor. Soc. Japan)
- Shuman, F.G., 1957: Predictive consequences of certain physical inconsistencies in the geostrophic barotropic model. Monthly Weather Review., 85, 229-234.
- Shuman, F.G., and J.B. Hovermale, 1968: An operational 6-layer primitive equation model. J. of Applied Meteor., 7, 525-547.
- Stackpole, John D., 1968: Operational Prediction Models at the National Meteorological Center, Tech. Memo., Development Division, National Meteorological Center, Suitland, Maryland, 34 pp.
- Syōno, S., 1963: Relaxation Methods for Engineers (in Japanese). Asakuwa Book Co., Tokyo, Japan, 185 pp.
- Wachspress, Eugene, L., 1966: Iterative Solution of Elliptic Systems. Prentice-Hall, Englewood Cliffs, N.J., 299 pp.
- Wilkinson, J.H., 1965: The Algebraic Eigenvalue Problem. Clarendon Press, Oxford, 662 pp.

## Appendix A

### Governing Hydrodynamical Equations

A set of equations is derived appropriate for flow in the planetary boundary layer and extending over horizontal distances the order of  $10^3$  km. The time scale of interest is that characterized by low frequency internal waves, the order of 10 hours. The model is designed to include the effects of rotation, moisture advection, eddy transport, and orography. The effects of latent heat release and radiation, however, are not included. The equations are developed in terms of coordinates on the polar stereographic projection to facilitate the handling of meteorological data. The equations take the following form:

$$\frac{du}{dt} = fv - m \frac{1}{\rho} \frac{\partial p}{\partial x} + \frac{\partial}{\partial z} (K_M \frac{\partial u}{\partial z}) \quad (\text{A} - 1)$$

$$\frac{dv}{dt} = -fu - m \frac{1}{\rho} \frac{\partial p}{\partial y} + \frac{\partial}{\partial z} (K_M \frac{\partial v}{\partial z}) \quad (\text{A} - 2)$$

$$\frac{dw}{dt} = - \frac{1}{\rho} \frac{\partial p}{\partial z} - g \quad (\text{A} - 3)$$

$$\frac{1}{\rho} \frac{dp}{dt} = - m \left( \frac{\partial u}{\partial x} + \frac{\partial v}{\partial y} \right) - \frac{\partial w}{\partial z} \quad (\text{A} - 4)$$

$$\frac{d\theta}{dt} = \frac{\partial}{\partial z} (K_H \frac{\partial \theta}{\partial z}) \quad (\text{A} - 5)$$

$$\frac{dq}{dt} = 0 \quad (\text{A - 6})$$

$$p = \rho RT \quad (\text{A - 7})$$

$$\theta = T \left( \frac{p_0}{p} \right)^{\kappa} \quad (\text{A - 8})$$

$$m = \frac{1 + \sin 60^\circ}{1 + \sin \frac{\phi}{2}} \quad (\text{A - 9})$$

and

$$\frac{d}{dt} = \frac{\partial}{\partial t} + m(u \frac{\partial}{\partial x} + v \frac{\partial}{\partial y}) + w \frac{\partial}{\partial z} \quad (\text{A - 10})$$

The symbols used are:

- x,y : horizontal cartesian coordinates on polar stereographic projection
- z : geometric height above the projection
- t : time
- m : map scale factor
- u : x - component of velocity
- v : y - component of velocity
- w : z - component of velocity
- p : pressure
- $\rho$  : density
- T : absolute temperature
- $\theta$  : potential temperature

- $q$  : specific humidity  
 $K_M$  : eddy coefficient of viscosity  
 $K_H$  : eddy coefficient of heat conductivity  
 $\kappa$  :  $R/c_p$ , ratio of gas constant for dry air to specific heat of air at constant pressure  
 $g$  : acceleration of gravity  
 $P_0$  : reference pressure ( = 1000 mb)  
 $\phi$  : latitude  
 $f$  : Coriolis parameter

The dependent variables are decomposed into a basic state denoted by  $(\bar{\quad})$  and a perturbation upon the basic state denoted by  $(\quad)'$ .

$$\begin{aligned}
 p &= \bar{p}(z) + p' & u &= u' \\
 \rho &= \bar{\rho}(z) + \rho' & v &= v' \\
 T &= \bar{T}(z) + T' & w &= w' \\
 \theta &= \bar{\theta}(z) + \theta' & q &= q'
 \end{aligned}
 \tag{A - 11}$$

The basic state chosen for this model is the distribution depicted by the U.S. Standard Atmosphere. The essential properties of this state are:

- (1) linear decrease of temperature with altitude at rate of  $6.5^\circ\text{C km}^{-1}$ ,
- (2) atmosphere is dry and obeys the perfect gas law,
- (3) atmosphere is at rest and in hydrostatic equilibrium.

The basic state satisfies the governing equations except for (A - 5). When the basic state variables are substituted into (A - 5), one finds

$$\frac{\partial}{\partial z} (K_H \frac{\partial \bar{\theta}}{\partial z}) = 0. \quad (\text{A} - 12)$$

From the definition of the U.S. Standard Atmosphere, the vertical distribution of  $\bar{\theta}$  is found to be

$$\frac{\partial \bar{\theta}}{\partial z} = 3.26 \left( \frac{1000}{\bar{p}} \right) \text{ } ^\circ\text{C km}^{-1} \quad (\text{A} - 13)$$

when  $\bar{p}$  is expressed in millibars. Consequently, (A - 12) is not valid except for some special distribution of  $K_H$ . However, if one uses typical values of  $K_H$  ( $\sim 10^4 \text{ cm}^2 \text{ sec}^{-1}$ ), appropriate to the lower atmosphere, then the order of magnitude of the term in (A - 12) is  $10^{-4} \text{ } ^\circ\text{C hr}^{-1}$  and can be justifiably neglected in the governing equations.

The governing equations in terms of the perturbations are

$$\frac{du}{dt} = fv - m \frac{1}{\rho} \frac{\partial p'}{\partial x} + \frac{\partial}{\partial z} (K_M \frac{\partial u}{\partial z}) + 0(10^{-4} \text{ m sec}^{-2}) \quad (\text{A} - 14)$$

$$\frac{dv}{dt} = -fu - m \frac{1}{\rho} \frac{\partial p'}{\partial y} + \frac{\partial}{\partial z} (K_M \frac{\partial v}{\partial z}) + 0(10^{-4} \text{ m sec}^{-2}) \quad (\text{A} - 15)$$

$$\frac{dw}{dt} = -\frac{1}{\rho} \frac{\partial p'}{\partial z} - g \frac{\rho'}{\rho} + 0(10^{-1} \text{ m sec}^{-2}) \quad (\text{A} - 16)$$

$$\frac{1}{\rho} \frac{d\rho'}{dt} = -\frac{w}{\rho} \frac{\partial \bar{\rho}}{\partial z} - m \left( \frac{\partial u}{\partial x} + \frac{\partial v}{\partial y} \right) - \frac{\partial w}{\partial z} + 0(10^{-7} \text{ sec}^{-1}) \quad (\text{A} - 17)$$

$$\frac{d\theta'}{dt} = -w \frac{\partial \bar{\theta}}{\partial z} + \frac{\partial}{\partial z} (K_H \frac{\partial \theta'}{\partial z}) + 0(10^{-4} \text{ } ^\circ\text{C hr}^{-1}) \quad (\text{A} - 18)$$

$$\frac{dq}{dt} = 0 \quad (\text{A - 19})$$

$$\frac{p'}{\gamma \bar{p}} = \frac{p'}{\bar{p}} + \frac{\theta'}{\bar{\theta}} + O(10^{-2}) \quad (\text{A - 20})$$

where  $\gamma = c_p/c_v$ , the ratio of the specific heat of air at constant pressure to the specific heat at constant volume. The magnitude of the highest order terms neglected in each equation is denoted by  $O(\ )$ , translated as "order of." Since the perturbations of the velocity components and specific humidity represent the complete description of these variables, the primes are dropped without confusion in notation.

The quotient  $(p'/\bar{\rho})$  appears naturally in the three momentum equations and a new variable is introduced in place of pressure,

$$\varphi = p'/\bar{\rho} \quad (\text{A - 21})$$

It is a simple matter to incorporate this variable into (A - 14) and (A - 15). Some manipulation is necessary, however, for incorporation into (A - 16) and (A - 20). The following identity can be established by use of (A - 21) and the rule for quotient differentiation:

$$\frac{1}{\bar{\rho}} \frac{\partial p'}{\partial z} = \frac{\partial \varphi}{\partial z} + \frac{p'}{\bar{\rho}^2} \frac{\partial \bar{\rho}}{\partial z} \quad (\text{A - 22})$$

Equation (A - 16) then takes the form

$$\frac{dw}{dt} = - \frac{\partial \varphi}{\partial z} - g \frac{p'}{\bar{p}} - \frac{\varphi}{\bar{\rho}} \frac{\partial \bar{\rho}}{\partial z} \quad (\text{A - 23})$$

Equation (A - 20) can be expressed as

$$\frac{\varphi}{c^2} = \frac{\rho'}{\rho} + \frac{\theta'}{\theta} \quad (\text{A - 24})$$

where  $c^2 = \gamma R \bar{T}$ , the speed of sound squared. Substitution of (A - 24) into (A - 23) gives

$$\frac{dw}{dt} = - \frac{\partial \varphi}{\partial z} - \frac{g\varphi}{c^2} + g \frac{\theta'}{\theta} - \frac{\varphi}{\rho} \frac{\partial \bar{\rho}}{\partial z} \quad (\text{A - 25})$$

Using the definitions of the U.S. Standard Atmosphere, one finds

$$\begin{aligned} \frac{1}{\rho} \frac{\partial \bar{\rho}}{\partial z} &= - \frac{1}{T} \left( \frac{\partial \bar{T}}{\partial z} + g/R \right) \\ &= -1.135 \text{ g}/c^2 \end{aligned} \quad (\text{A - 26})$$

where 1.135 is the numerical value of

$$\left( \frac{g}{R} + \frac{\partial \bar{T}}{\partial z} \right) / \left( \frac{g}{R} - \Gamma_d \right)$$

$\Gamma_d$  ( $= g/c_p$ ) denoting the dry adiabatic lapse rate. Thus (A - 16) finally can be written as

$$\frac{dw}{dt} = - \frac{\partial \varphi}{\partial z} + g \frac{\theta'}{\theta} + 0(10^{-1} \text{ m sec}^{-2}) \quad (\text{A - 27})$$

At this point, it is convenient to introduce a coordinate transformation which assists in handling the orographic features. An "orographic coordinate," first used by Sasaki et al. (1967), takes the place of  $z$  and is defined as follows:

$$\sigma = z - H(x,y) \quad (\text{A - 28})$$

where  $H(x,y)$  represents terrain elevation above mean sea level. In order to examine the dependent variables in  $x, y, \sigma, t$  coordinates, we transform the governing equations by use of the following identities:

$$\frac{\partial}{\partial x} \Big|_z = \frac{\partial}{\partial x} \Big|_\sigma - \frac{\partial H}{\partial x} \frac{\partial}{\partial \sigma}$$

$$\frac{\partial}{\partial y} \Big|_z = \frac{\partial}{\partial y} \Big|_\sigma - \frac{\partial H}{\partial y} \frac{\partial}{\partial \sigma} \quad (\text{A - 29})$$

$$\frac{\partial}{\partial z} = \frac{\partial}{\partial \sigma}$$

The perturbation equations in the  $x, y, \sigma, t$  system are:

$$\dot{u} = fv - m \frac{\partial \varphi}{\partial x} + m \frac{\partial H}{\partial x} \frac{\partial \varphi}{\partial \sigma} + \frac{\partial}{\partial \sigma} (K_M \frac{\partial u}{\partial \sigma}) \quad (\text{A - 30})$$

$$\dot{v} = -fu - m \frac{\partial \varphi}{\partial y} + m \frac{\partial H}{\partial y} \frac{\partial \varphi}{\partial \sigma} + \frac{\partial}{\partial \sigma} (K_M \frac{\partial v}{\partial \sigma}) \quad (\text{A - 31})$$

$$\dot{w} = -\frac{\partial \varphi}{\partial \sigma} + g \frac{\theta'}{\theta} \quad (\text{A - 32})$$

$$\frac{1}{\rho} \dot{\rho}' = -w^* \frac{1}{\rho} \frac{\partial \bar{\rho}}{\partial \sigma} - m \left( \frac{\partial u}{\partial x} + \frac{\partial v}{\partial y} \right) - \frac{\partial w^*}{\partial \sigma} \quad (\text{A - 33})$$

$$\dot{\theta}' = -w^* \frac{\partial \bar{\theta}}{\partial \sigma} + \frac{\partial}{\partial \sigma} (K_H \frac{\partial \theta'}{\partial \sigma}) \quad (\text{A - 34})$$

$$\dot{q} = 0 \quad (\text{A - 35})$$

$$\frac{\varphi}{c^2} = \frac{\rho'}{\rho} + \frac{\theta'}{\theta} \quad (\text{A - 36})$$

$$w^* = w - m(u \frac{\partial H}{\partial x} + v \frac{\partial H}{\partial y}) \quad (\text{A - 37})$$

where all partial derivatives are in the  $x, y, \sigma, t$  system, i.e.,  $\frac{\partial \varphi}{\partial x}$  implies the change of  $\varphi$  with respect to  $x$  when  $y, \sigma,$  and  $t$  are held constant and

$$(\dot{\quad}) = \left\{ \frac{\partial}{\partial t} + mu \frac{\partial}{\partial x} + mv \frac{\partial}{\partial y} + w^* \frac{\partial}{\partial \sigma} \right\} (\quad) \quad (\text{A - 38})$$

The "vertical velocity" in the  $x, y, \sigma, t$  system is denoted by  $w^*$ . This measures the change of a fluid parcel's  $\sigma$  coordinate with time, i.e., it represents the substantial or material derivative of  $\sigma$ . The vertical velocity,  $w$ , approaches  $w^*$  when the mountain slopes are small and/or the horizontal wind speed is small. The maximum slopes of the terrain used in this study are the order of  $10^{-3}$ . A map of the orographic features is shown in Fig. 1.

Equations (A - 30) through (A - 38) are now non-dimensionalized. Each variable, both dependent and independent, is set equal to the product of a scale quantity (dimensional constant) and a non-dimensional quantity. The scale quantity is chosen in such a way that the non-dimensional variable is the order of magnitude 1. A superscript " $\wedge$ " is used to designate the non-dimensional variable. A list of the variables is as follows:

$$u = V_0 \hat{u}$$

$$v = V_0 \hat{v}$$

$$w = \frac{Z_0 V_0}{L_0} \hat{w} = w_0 \hat{w}$$

$$w^* = w_0 \hat{w}^*$$

$$q = q_0 \hat{q}$$

$$\varphi = f_0 V_0 L_0 \hat{\varphi} = \varphi_0 \hat{\varphi}$$

$$\theta' = \theta_0 \hat{\theta}$$

$$\rho' = \rho_0 \hat{\rho}$$

$$H = H_0 \hat{h}$$

$$K_M = K_{MO} \hat{K}_M$$

$$K_H = K_{HO} \hat{K}_H$$

$$x = L_0 \hat{x}$$

$$y = L_0 \hat{y}$$

$$\sigma = Z_0 \hat{\sigma}$$

$$t = \frac{L_0}{V_0} \hat{t} = t_0 \hat{t}$$

where

$L_0 = 10^6$  m: horizontal length scale       $V_0 = 10$  m sec<sup>-1</sup>: horizontal velocity  
 $Z_0 = 10^3$  m: boundary layer depth       $\theta_0 = 10^\circ$  C: perturbation temperature  
 $H_0 = 10^3$  m: mountain height above M.S.L.       $\rho_0 = 10^{-1}$  kg m<sup>-3</sup>: perturbation density  
 $K_{MO} = 1$  m<sup>2</sup> sec<sup>-1</sup>: eddy coefficient of momentum       $w_0 = 10^{-2}$  m sec<sup>-1</sup>: vertical velocity  
 $K_{HO} = 1$  m<sup>2</sup> sec<sup>-1</sup>: eddy coefficient of heat       $q_0 = 10$  o/oo : specific humidity  
 $f_0 = 10^{-4}$  sec<sup>-1</sup>: Coriolis parameter       $t_0 = 10^5$  sec : time

When the scaled representation of the variables is substituted into the governing equations, the equations take the following form:

$$Ro \frac{\partial \hat{u}}{\partial \hat{t}} = \hat{v} - \frac{\partial \hat{\varphi}}{\partial \hat{x}} + \frac{\partial \hat{h}}{\partial \hat{x}} \frac{\partial \hat{\varphi}}{\partial \hat{\sigma}} + \Lambda_M \frac{\partial}{\partial \hat{\sigma}} \left( \hat{K}_M \frac{\partial \hat{u}}{\partial \hat{\sigma}} \right) \quad (\text{A - 39})$$

$$Ro \frac{\partial \hat{v}}{\partial \hat{t}} = -\hat{u} - \frac{\partial \hat{\varphi}}{\partial \hat{y}} + \frac{\partial \hat{h}}{\partial \hat{y}} \frac{\partial \hat{\varphi}}{\partial \hat{\sigma}} + \Lambda_M \frac{\partial}{\partial \hat{\sigma}} \left( \hat{K}_M \frac{\partial \hat{v}}{\partial \hat{\sigma}} \right) \quad (\text{A - 40})$$

$$\frac{Ro}{r} \dot{\hat{w}} = - \frac{\partial \hat{\phi}}{\partial \hat{\sigma}} + \mu \hat{\theta} \quad (\text{A - 41})$$

$$\dot{\hat{\theta}} = - \hat{w}^* \bar{\theta}_{\sigma} + \Lambda_H \frac{\partial}{\partial \hat{\sigma}} \left( K_H \frac{\partial \hat{\theta}}{\partial \hat{\sigma}} \right) \quad (\text{A - 42})$$

$$\left( \frac{\rho_0}{\rho} \right) \dot{\hat{p}} = - \hat{w}^* \bar{\rho}_{\sigma} - \left( \frac{\partial \hat{u}}{\partial \hat{x}} + \frac{\partial \hat{v}}{\partial \hat{y}} + \frac{\partial \hat{w}^*}{\partial \hat{\sigma}} \right) \quad (\text{A - 43})$$

$$\dot{\hat{q}} = 0 \quad (\text{A - 44})$$

$$\hat{\psi} = \lambda \hat{p} + \beta \hat{\theta} \quad (\text{A - 45})$$

$$\hat{w}^* = \hat{w} - \hat{u} \frac{\partial \hat{h}}{\partial \hat{x}} - \hat{v} \frac{\partial \hat{h}}{\partial \hat{y}} \quad (\text{A - 46})$$

where

$$(\dot{\quad}) = \left\{ \frac{\partial}{\partial \hat{t}} + \hat{u} \frac{\partial}{\partial \hat{x}} + \hat{v} \frac{\partial}{\partial \hat{y}} + \hat{w}^* \frac{\partial}{\partial \hat{\sigma}} \right\} (\quad) \quad (\text{A - 47})$$

and the map scale factor has been incorporated into the horizontal space derivatives for convenience of notation, i.e., there is an implied multiplication by "m" whenever a horizontal space derivative appears. The non-dimensional numbers appearing in equations (A - 39) through (A - 46) are defined as follows:

$$Ro = \frac{V_0}{f_0 L_0} = 10^{-1} \quad (\text{Rossby number})$$

$$\bar{\theta}_{\sigma} = \frac{Z_0}{\theta_0} \frac{\partial \bar{\theta}}{\partial \hat{\sigma}} \approx 3.5 \times 10^{-1}$$

$$\mu = Ro \cdot \frac{\theta_0}{\theta} \frac{g Z_0}{V_0^2} \approx 3.3 \times 10^{-1}$$

$$\bar{\rho}_{\sigma} = \frac{Z_0}{\rho} \frac{\partial \bar{\rho}}{\partial \hat{\sigma}} \approx 10^{-1}$$

$$\Lambda_M = \frac{K_{MO}}{f_0 Z_0^2} = 10^{-2}$$

$$\beta = \frac{c^2}{f_0 V_0 L_0} \frac{\theta_0}{\theta} \approx 3.3$$

$$\Lambda_H = \frac{K_{HO} \cdot L_0}{Z_0^2 V_0} = 10^{-1}$$

$$\lambda = \frac{c^2}{f_0 V_0 L_0} \frac{\rho_0}{\rho} \approx 10$$

$$r = \left( \frac{L_0}{Z_0} \right)^2 = 10^6$$

Equations (A - 39) through (A - 46) with the accompanying non-dimensional numbers provide immediate insight into the relative magnitude of each term. Since the variables have been scaled in a way such that the non-dimensional variables are of order 1, the scalar constants completely determine the magnitude of a given term. Consequently, the factor  $(Ro/r)$  in Eq. (A - 41), of order  $10^{-7}$ , implies that the vertical acceleration is approximately seven orders of magnitude smaller than the terms on the right hand side of (A - 41). This result is well known for atmospheric flow in which the horizontal scale of motion is much larger than the vertical scale (Ogura, 1963). Equivalently stated, the hydrostatic balance is a good approximation for this flow and Eq. (A - 41) is sensitive to error when used prognostically. Similarly, Eq. (A - 43) provides justification for the assumption of incompressibility.

As a consequence of the scale analysis and the arguments above, the set of governing equations assume the following form:

$$Ro \cdot \dot{u} = v - \frac{\partial \phi}{\partial x} + \mu \frac{\partial h}{\partial x} \theta + \Lambda_M \frac{\partial}{\partial \sigma} \left( K_M \frac{\partial u}{\partial \sigma} \right) \quad (A - 48)$$

$$Ro \cdot \dot{v} = -u - \frac{\partial \phi}{\partial y} + \mu \frac{\partial h}{\partial y} \theta + \Lambda_M \frac{\partial}{\partial \sigma} \left( K_M \frac{\partial v}{\partial \sigma} \right) \quad (A - 49)$$

$$0 = -\frac{\partial \phi}{\partial \sigma} + \mu \theta \quad (A - 50)$$

$$\dot{\theta} = -w^* \bar{\theta}_\sigma + \Lambda_H \frac{\partial}{\partial \sigma} \left( K_H \frac{\partial \theta}{\partial \sigma} \right) \quad (\text{A - 51})$$

$$0 = \frac{\partial u}{\partial x} + \frac{\partial v}{\partial y} + \frac{\partial w^*}{\partial \sigma} \quad (\text{A - 52})$$

$$\dot{q} = 0 \quad (\text{A - 53})$$

$$\psi = \lambda p + \beta \theta \quad (\text{A - 54})$$

$$w^* = w - u \frac{\partial h}{\partial x} - v \frac{\partial h}{\partial y} \quad (\text{A - 55})$$

where, for convenience in future reference, the " $\wedge$ " has been dropped and all variables will be assumed non-dimensional unless otherwise specified. Also, the hydrostatic relation, (A - 50) has been used to simplify (A - 48) and (A - 49).

These equations admit low frequency internal gravity waves. To verify this point, a frequency analysis similar to that developed by Monin and Obukhov (1958) is used. The governing equations are linearized and the static stability,  $\bar{\theta}_\sigma$ , is assumed constant. Also the flow is considered two dimensional, i.e., all variations in the y-direction vanish. This last assumption does not limit the value of the frequency analysis. The perturbations of the meteorological variables are expressed in Fourier representation, viz.,

$$\begin{aligned} u &= A(k, l, \omega) \exp\{i(kx + lz - \omega t)\} \\ v &= B(k, l, \omega) \exp\{i(kx + lz - \omega t)\} \\ &\text{etc.} \end{aligned} \quad (\text{A - 56})$$

where A and B are amplitudes of the waves in the u and v spectrum, respectively. In general, each field will possess more than one characteristic wave, but

since this analysis is linear, the operation on a particular wave serves to demonstrate the general technique. In the representation above,

$$k = \frac{2\pi L_0}{L_x}, \quad l = \frac{2\pi Z_0}{L_z}, \quad \omega = \frac{2\pi t_0}{T} \quad (\text{A - 57})$$

Substitution of (A - 56) into (A - 48) through (A - 55) gives the frequency equation:

$$\omega = k \pm Ro^{-1} \sqrt{1 + \mu \bar{\theta}_\sigma \cdot Ro \cdot \left(\frac{L_0}{Z_0}\right) \frac{L_z}{L_x}} \quad (\text{A - 58})$$

Internal gravity wave motion with periods the order of 10 hr are contained in this spectrum. Also, the acoustic waves and external gravity waves are excluded.

A finite difference analog of the governing set is formulated for use in the initialization process. The space operations are defined as follows:

$$\nabla_x \bar{\Phi}_0]_{ijk} = \frac{(\bar{\Phi}_0)_{i+1} - (\bar{\Phi}_0)_{i-1}}{2\Delta s} \quad (\text{A - 59})$$

$$\nabla_y \bar{\Phi}_0]_{ijk} = \frac{(\bar{\Phi}_0)_{j+1} - (\bar{\Phi}_0)_{j-1}}{2\Delta s} \quad (\text{A - 60})$$

$$\nabla_\sigma \bar{\Phi}_0]_{ijk} = \frac{(\bar{\Phi}_0)_{k+1} - (\bar{\Phi}_0)_{k-1}}{2\Delta\sigma} \quad (\text{A - 61})$$

where  $i$ ,  $j$ , and  $k$  are the grid indices along the  $x$ ,  $y$ , and  $\sigma$  axes, respectively. The grid spacing in the horizontal and vertical are represented by  $\Delta s$  and  $\Delta\sigma$ . Subscripting of variables is designed to reduce cluttered notation. For derivative evaluation at  $i$ ,  $j$ , or  $k$ , only those subscripts different from  $i$ ,  $j$ ,

or  $k$  are identified.

When a forward time step is used in conjunction with the above space differencing, Equations (A - 48) through (A - 54) assume the following form:

$$\frac{Ro}{\Delta t} (u_1 - u_0) = \begin{cases} -Ro (u_0 \nabla_x u_0 + v_0 \nabla_y u_0 + w_0^* \nabla_\sigma u_0) \\ +v_0 - \nabla_x \varphi_0 + \mu \nabla_x h \cdot \theta_0 + \Lambda_M \nabla_\sigma (K_M \nabla_\sigma u_0) \end{cases} \quad (A - 62)$$

$$\frac{Ro}{\Delta t} (v_1 - v_0) = \begin{cases} -Ro (u_0 \nabla_x v_0 + v_0 \nabla_y v_0 + w_0^* \nabla_\sigma v_0) \\ -u_0 - \nabla_y \varphi_0 + \mu \nabla_y h \cdot \theta_0 + \Lambda_M \nabla_\sigma (K_M \nabla_\sigma v) \end{cases} \quad (A - 63)$$

$$\frac{\theta_1 - \theta_0}{\Delta t} = \begin{cases} - (u_0 \nabla_x \theta_0 + v_0 \nabla_y \theta_0 + w_0^* \nabla_\sigma \theta_0) \\ - w_0^* \bar{\theta}_\sigma + \Lambda_H \nabla_\sigma (K_H \nabla_\sigma \theta_0) \end{cases} \quad (A - 64)$$

$$0 = \nabla_x u_0 + \nabla_y v_0 + \nabla_\sigma w_0^* \quad (A - 65)$$

$$\frac{q_1 - q_0}{\Delta t} = - (u_0 \nabla_x q_0 + v_0 \nabla_y q_0 + w_0^* \nabla_\sigma q_0) \quad (A - 66)$$

$$\varphi_0 = \lambda \rho_0 + \beta \theta_0 \quad (A - 67)$$

This finite difference scheme has definite limitations when used to forecast for more than several time steps. The forward time and centered

space formulation suffers from computational instability (Richtmyer, 1967), i.e., an initial field will tend to amplify unrealistically as time proceeds. However, when used to forecast over only a few time steps this amplification is not prohibitive.

This scheme possesses a feature that warrants its use for the initialization problem. Namely, there is no wavelength discrimination. Some of the sophisticated schemes such as Lax-Wendroff (see Richtmyer, 1963) can be rendered computationally stable, but they often damp certain wavelengths and, in general, possess artificial diffusion. Sasaki (1969) has shown that the diffusive character of the Lax-Wendroff scheme is injurious to the objective analysis.

## APPENDIX B

### CONVERGENCE OF ITERATION SCHEME

The convergence properties of the iterative method proposed in Chapter II are examined. The examination follows the pattern proposed by Frankel (1950) and requires the linearization of the difference equations. This investigation of convergence does not include the specific humidity field. Since the moisture equation describes only the advection of specific humidity, the convergence of  $u_0$  and  $v_0$  will most likely imply the convergence of  $q_0$ .

We adopt the following notation:

$$\Delta u_0^{(p)} = u_0^{(p)} - u_0 \quad (\text{B - 1})$$

$$\Delta v_0^{(p)} = v_0^{(p)} - v_0 \quad (\text{B - 2})$$

$$\Delta \theta_0^{(p)} = \theta_0^{(p)} - \theta_0 \quad (\text{B - 3})$$

where  $\Delta u_0^{(p)}$  is used to denote the error in the u-field at grid point (i, j, k) for the pth iteration and similarly for the other meteorological variables. The iterative scheme is convergent if

$$\lim_{p \rightarrow \infty} \{ \Delta u_0^{(p)}, \Delta v_0^{(p)}, \Delta \theta_0^{(p)} \} \rightarrow 0$$

Since the analysis equations are coupled, all three variables must either converge or all three must diverge.

Equations (7) - (9) and (14) - (16) are expressed as explicit functions of  $u_0$ ,  $v_0$ , and  $\theta_0$  and  $u_0^{(p)}$ ,  $v_0^{(p)}$ , and  $\theta_0^{(p)}$ , respectively. This is accomplished by substitution from (A - 62) through (A - 67). The equation set (7) - (9) is then subtracted from (14) - (16) to get alternate forms of the residue equations, namely,

$$A_{11} \Delta u_0^{(p)} + A_{12} \Delta v_0^{(p)} + A_{13} \Delta \theta_0^{(p)} = R_u^{(p)} \quad (B - 4)$$

$$A_{21} \Delta u_0^{(p)} + A_{22} \Delta v_0^{(p)} + A_{23} \Delta \theta_0^{(p)} = R_v^{(p)} \quad (B - 5)$$

$$A_{31} \Delta u_0^{(p)} + A_{32} \Delta v_0^{(p)} + A_{33} \Delta \theta_0^{(p)} = R_\theta^{(p)} \quad (B - 6)$$

where the operators  $A_{ij}$  are given in Table 1. The right hand sides of (B - 4) through (B - 6) can be expressed as functions of  $\Delta u_0^{(p)}$ ,  $\Delta v_0^{(p)}$ ,  $\Delta \theta_0^{(p)}$ ,  $\Delta u_0^{(p+1)}$ , etc., by using (18) - (20). The system can then be written

$$(1 + \alpha_u \cdot A_{11}) \Delta u_0^{(p)} + \alpha_u A_{12} \Delta v_0^{(p)} + \alpha_u A_{13} \Delta \theta_0^{(p)} = \Delta u_0^{(p+1)} \quad (B - 7)$$

$$\alpha_v A_{21} \Delta u_0^{(p)} + (1 + \alpha_v A_{22}) \Delta v_0^{(p)} + \alpha_v A_{23} \Delta \theta_0^{(p)} = \Delta v_0^{(p+1)} \quad (B - 8)$$

$$\alpha_\theta A_{31} \Delta u_0^{(p)} + \alpha_\theta A_{32} \Delta v_0^{(p)} + (1 + \alpha_\theta A_{33}) \Delta \theta_0^{(p)} = \Delta \theta_0^{(p+1)} \quad (B - 9)$$

Using matrix notation, we write

$$\Delta \vec{V}^{(p+1)} = M \Delta \vec{V}^{(p)} \quad (B - 10)$$

where

$$\Delta \vec{V}^{(p)} = \begin{bmatrix} \Delta u_0^{(p)} \\ \Delta v_0^{(p)} \\ \Delta \theta_0^{(p)} \end{bmatrix}, \quad M = \begin{bmatrix} (1 + \alpha_u A_{11}) & \alpha_u A_{12} & \alpha_u A_{13} \\ \alpha_v A_{21} & (1 + \alpha_v A_{22}) & \alpha_v A_{23} \\ \alpha_\theta A_{31} & \alpha_\theta A_{32} & (1 + \alpha_\theta A_{33}) \end{bmatrix} \quad (B - 11)$$

The matrix equation (B - 10) relates the error at the  $(p+1)$ st stage to the error at the  $p$ th stage. To examine the convergence of the iterative scheme, we assume that the guess fields (first approximation) have the following errors,

$$\Delta u_0^{(1)}(x, y, \sigma) = B_{\ell, m, n}^{(1)} \exp\left\{2\pi i \left[ \frac{\ell x}{N_x \Delta x} + \frac{m y}{N_y \Delta y} + \frac{n \sigma}{N_\sigma \Delta \sigma} \right]\right\}$$

$$\Delta v_0^{(1)}(x, y, \sigma) = C_{\ell, m, n}^{(1)} \exp\left\{2\pi i \left[ \frac{\ell x}{N_x \Delta x} + \frac{m y}{N_y \Delta y} + \frac{n \sigma}{N_\sigma \Delta \sigma} \right]\right\} \quad (B - 12)$$

$$\Delta \theta_0^{(1)}(x, y, \sigma) = D_{\ell, m, n}^{(1)} \exp\left\{2\pi i \left[ \frac{\ell x}{N_x \Delta x} + \frac{m y}{N_y \Delta y} + \frac{n \sigma}{N_\sigma \Delta \sigma} \right]\right\}$$

where B, C, and D are Fourier amplitudes and

$$x = r \Delta x \quad r = 0, 1, 2, \dots, N_x \quad (N_x = 12 \text{ for case study})$$

$$y = s \Delta y \quad s = 0, 1, 2, \dots, N_y \quad (N_y = 12 \text{ for case study})$$

$$\sigma = t \Delta \sigma \quad t = 0, 1, 2, \dots, N_\sigma \quad (N_\sigma = 8 \text{ for case study})$$

Letting

$$k_x = \frac{2\pi \ell}{N_x}$$

$$k_y = \frac{2\pi m}{N_y} \quad (\text{B} - 13)$$

$$k_\sigma = \frac{2\pi n}{N_\sigma}$$

we get

$$\Delta u_0^{(1)} = B_{\ell, m, n}^{(1)} \exp\{k_x r + k_y s + k_\sigma t\}$$

$$\Delta v_0^{(1)} = C_{\ell, m, n}^{(1)} \exp\{k_x r + k_y s + k_\sigma t\} \quad (\text{b} - 14)$$

$$\Delta \theta_0^{(1)} = D_{\ell, m, n}^{(1)} \exp\{k_x r + k_y s + k_\sigma t\}$$

The error at the  $p$ th stage can be found by repeated use of the matrix equation (B - 10). The iterative method is convergent (in general) only if

$$|\lambda(\ell, m, n)| < 1 \quad (\text{B} - 15)$$

is satisfied for all  $\ell, m, n$ , where  $|\lambda|$  represents the absolute value of the largest eigenvalue of  $M$ , i.e., the spectral radius.

It was found that initial errors with maximum wavelength, i.e.,  $\ell = m = n = 1$ , yielded the largest spectral radius. Consequently, in the testing procedure, these wavelengths were used. The relative magnitudes of the Lagrange multipliers must be determined such that the spectral radius is less than 1. Since there are effectively eight multipliers for this limited investigation, viz.,  $\alpha_1, \tilde{\alpha}, \nu_1, \tilde{\nu}, \gamma_1, \tilde{\gamma}, \epsilon$ , and  $\eta$ , the myriad possibilities prevents an exhaustive investigation. One method of procedure is developed by taking two multipliers non-zero and determining their ratio such that convergence results. In a step-wise manner, it is then possible to add the other multipliers, one at a time,

and determine a satisfactory set. Of course, the task is simplified somewhat by the fact that density of observation and reliability of data dictate the range on some multipliers. This method of attack is discussed in Chapter III when applied to the case study.

TABLE 1

## OPERATORS IN AMPLIFICATION MATRIX

$$\begin{aligned}
A_{11} &: \tilde{\gamma} - \eta \nabla_x^2 + \gamma_1 \left( \frac{\Delta t}{Ro} \right)^2 (\Lambda_M^2 \nabla_\sigma^4 + 1) \\
A_{12} &: -\eta \nabla_{xy}^2 \\
A_{13} &: \gamma_1 \left( \frac{\Delta t}{Ro} \right)^2 (\beta \nabla_y + \mu \nabla_x h \nabla_\sigma^2 - \mu \nabla_y h - \beta \Lambda_M \nabla_x \nabla_\sigma^2) \\
A_{21} &: -\eta \nabla_{xy}^2 \\
A_{22} &: \tilde{\gamma} - \eta \nabla_y^2 + \gamma_1 \left( \frac{\Delta t}{Ro} \right)^2 (\Lambda_M^2 \nabla_\sigma^4 + 1) \\
A_{23} &: \gamma_1 \left( \frac{\Delta t}{Ro} \right)^2 (-\beta \nabla_x + \mu \nabla_y h \nabla_\sigma^2 + \mu \nabla_x h - \beta \Lambda_M \nabla_y \nabla_\sigma^2) \\
A_{31} &: \gamma_1 \left( \frac{\Delta t}{Ro} \right)^2 (\Lambda_M [\beta \nabla_x + \mu \nabla_x h] \nabla_\sigma^2 - \beta \nabla_y - \mu \nabla_y h) \\
A_{32} &: \gamma_1 \left( \frac{\Delta t}{Ro} \right)^2 (\Lambda_M [\beta \nabla_y + \mu \nabla_y h] \nabla_\sigma^2 + \beta \nabla_x + \mu \nabla_x h) \\
A_{33} &: (\alpha_1 + v_1 \beta^2) (\Delta t \Lambda_H)^2 \nabla_\sigma^4 + \tilde{\alpha} + \tilde{\nu} \beta^2 \\
&+ \gamma_1 \left( \frac{\Delta t}{Ro} \right)^2 \beta (\mu \nabla_x h \nabla_x + \mu \nabla_y h \nabla_y) - \beta [\nabla_x^2 + \nabla_y^2] \\
&+ \gamma_1 \left( \frac{\Delta t}{Ro} \right)^2 (\mu \nabla_x h [\mu \nabla_x h - \beta \nabla_x] + \mu \nabla_y h [\mu \nabla_y h - \beta \nabla_y]) \\
&+ e (\mu^2 - \beta^2 \nabla_\sigma^2)
\end{aligned}$$

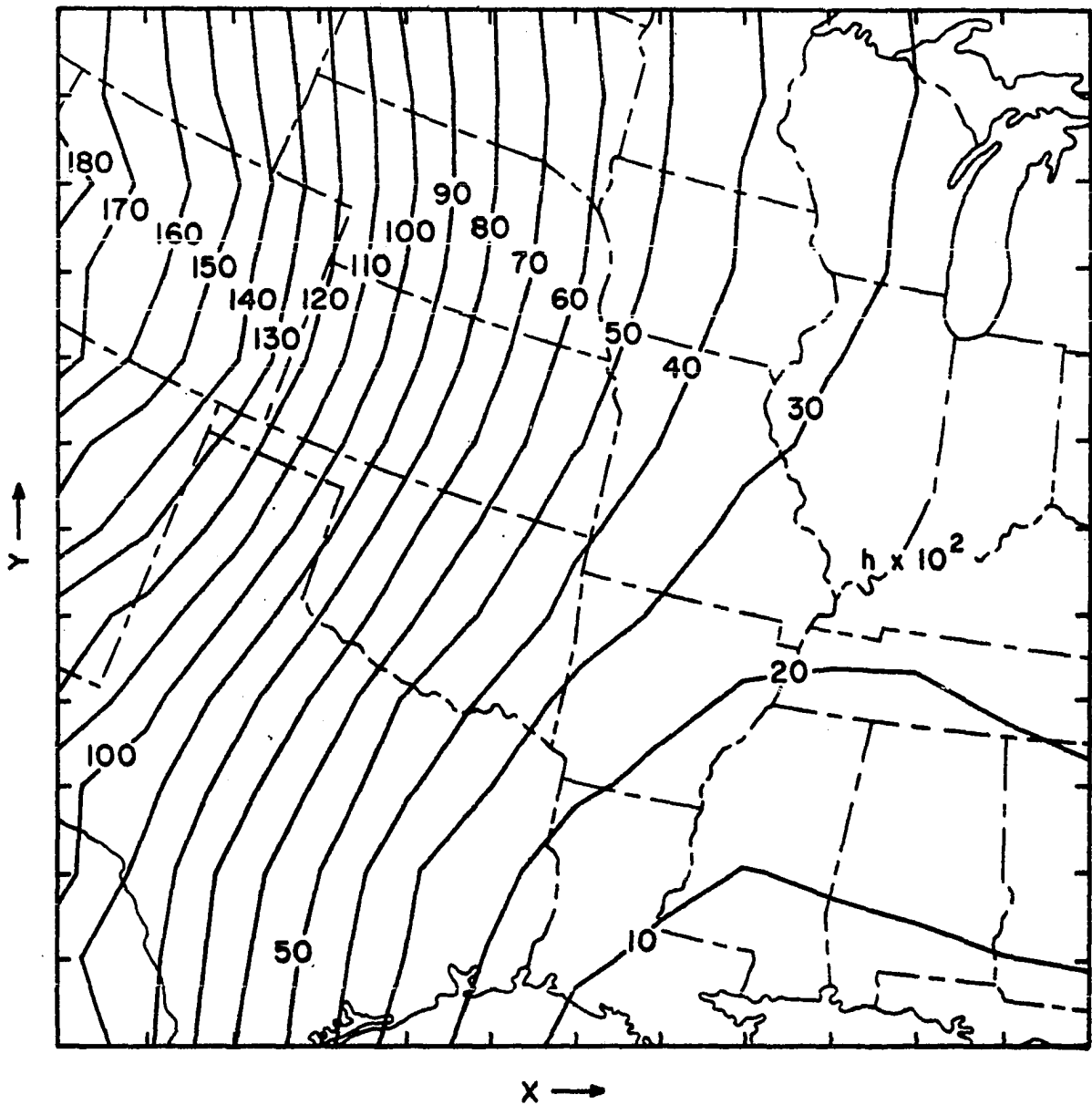


Fig. 1. Topographic features over the grid network in terms of non-dimensional height,  $h$ .

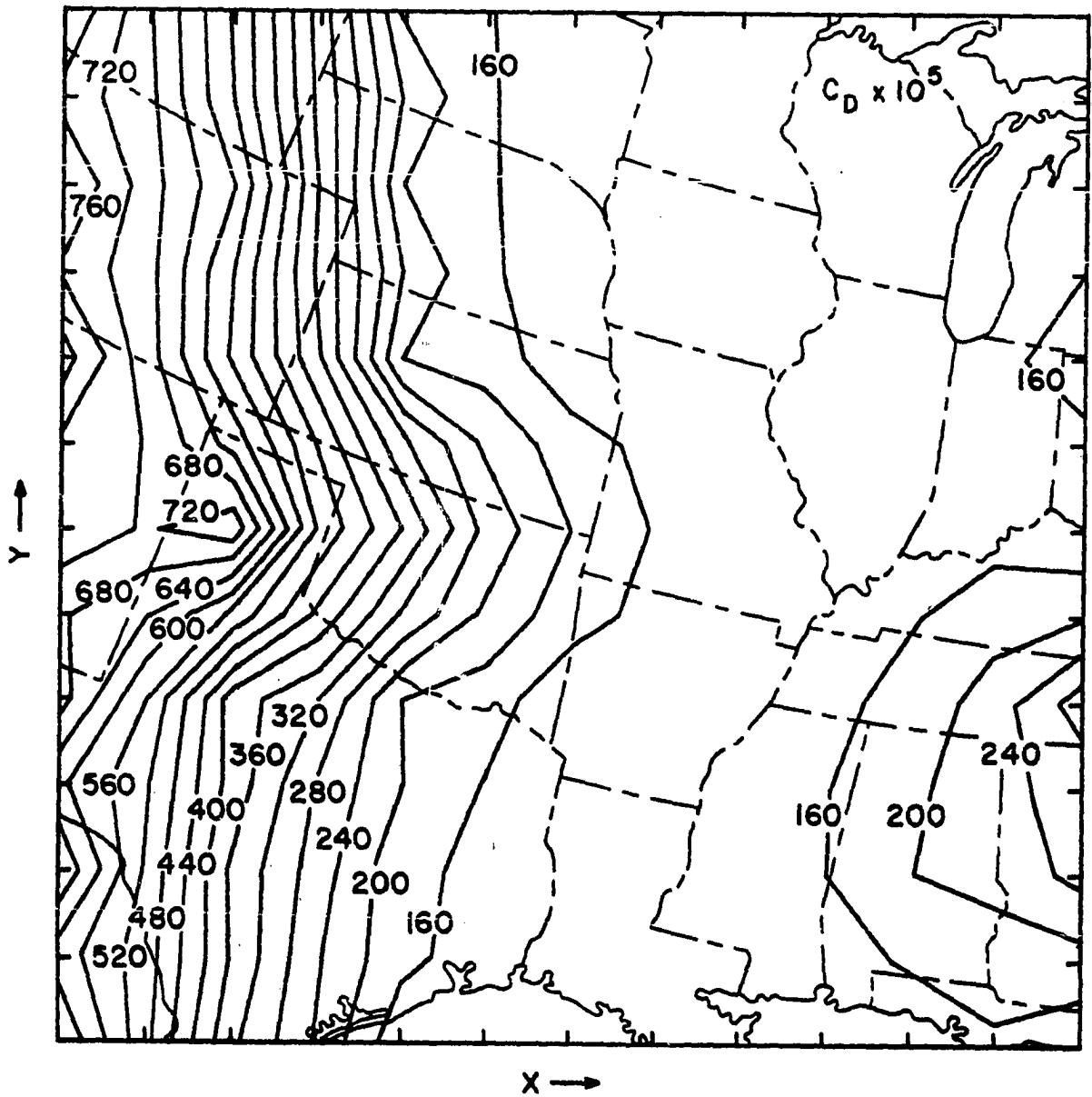


Fig. 2. Contours of the drag coefficient over the grid network.

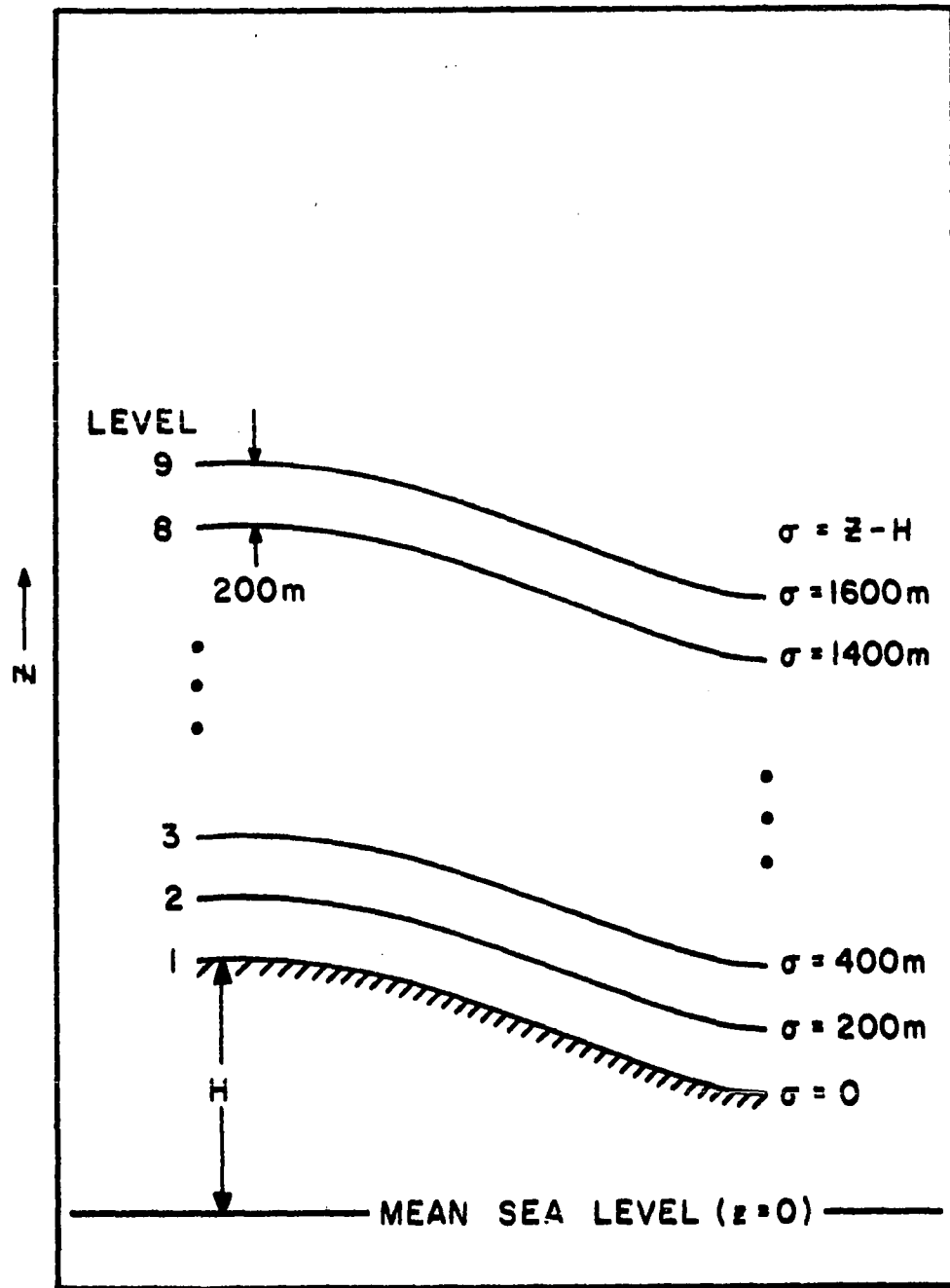


Fig. 3. Orographic coordinate surfaces.

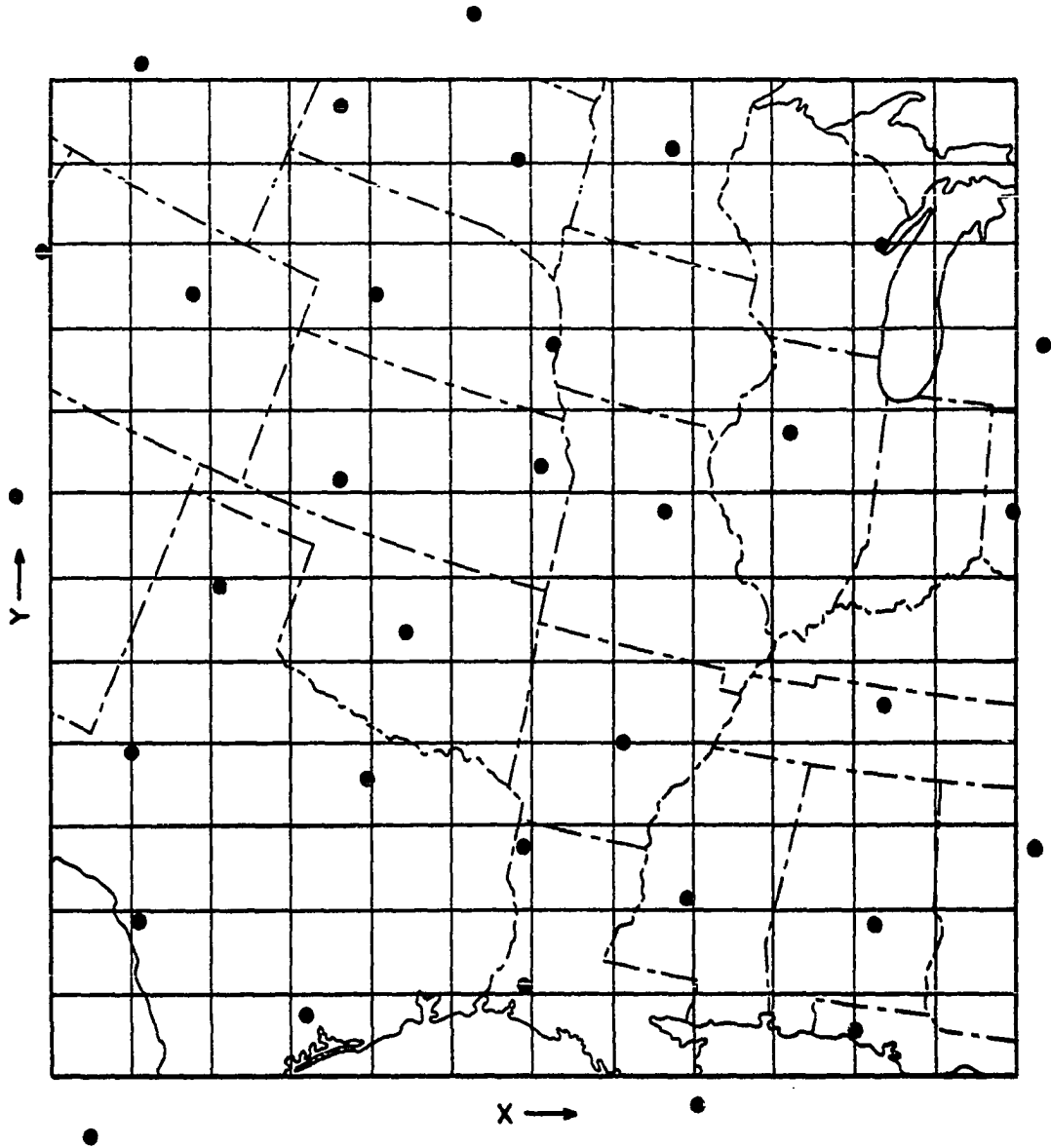


Fig. 4. Horizontal net of grid points and locations of the radiosonde stations.

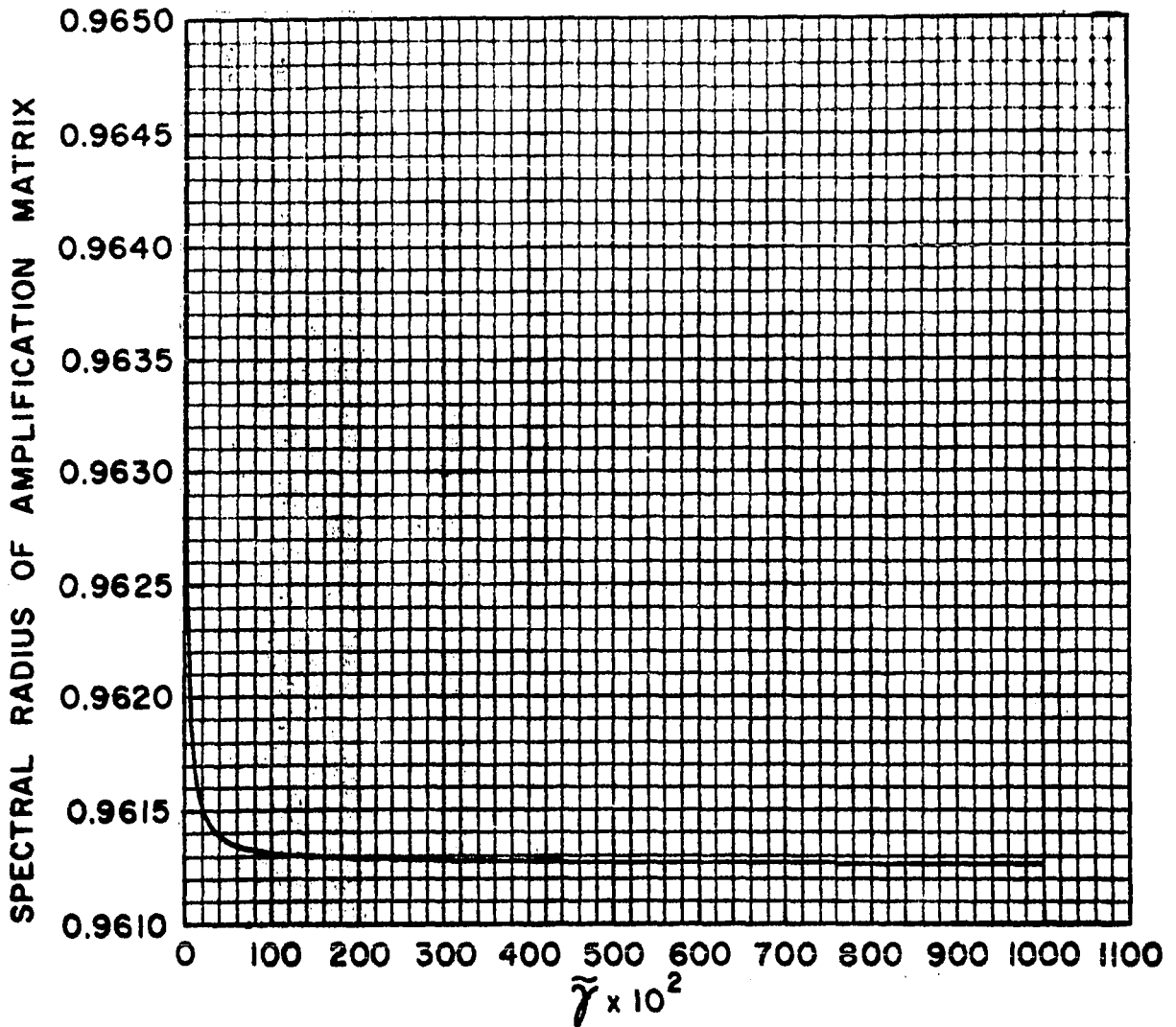


Fig. 5. Spectral radius of amplification matrix as a function of  $\tilde{\gamma}$ , the weight on observed wind.

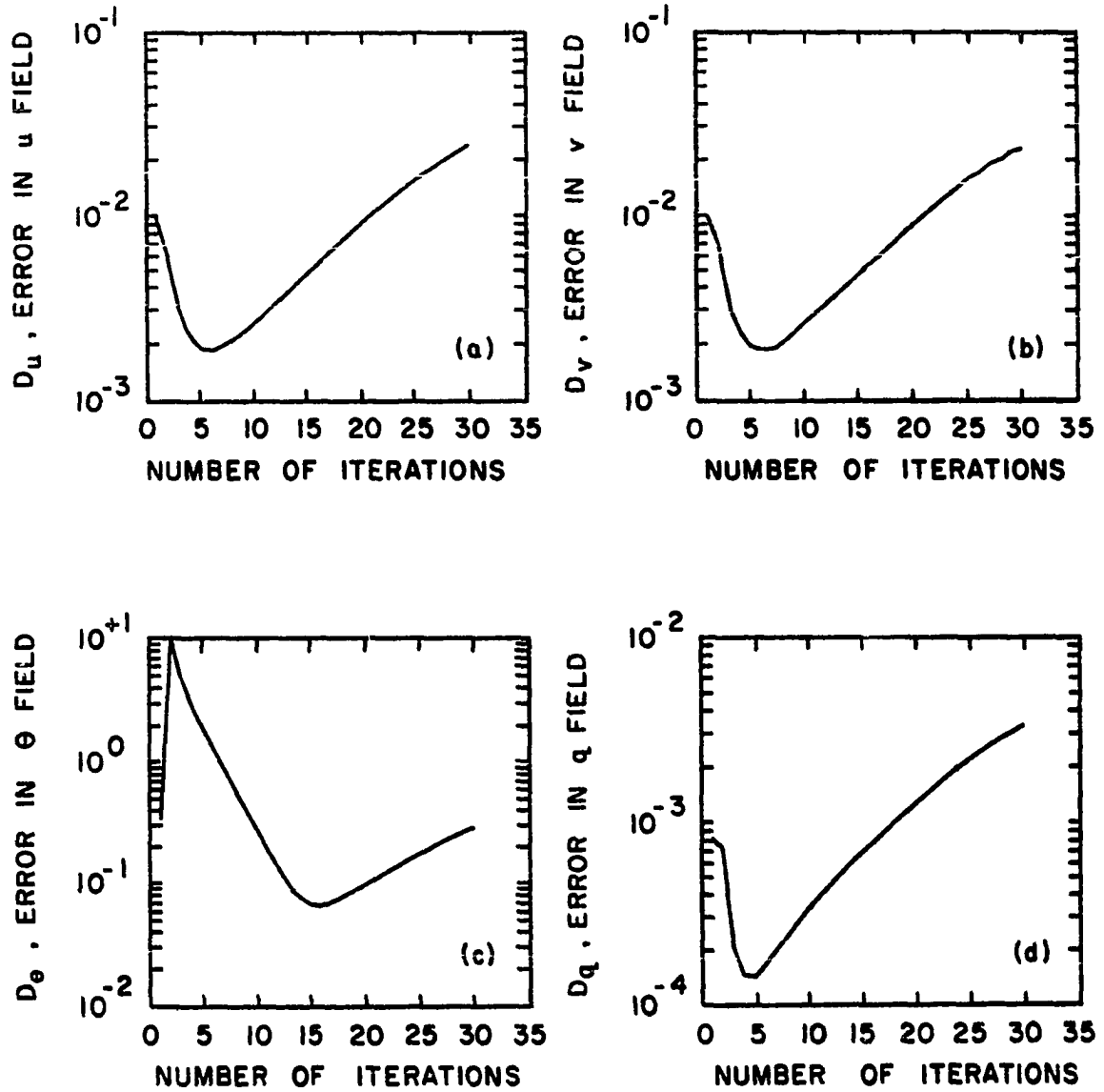


Fig. 6. Standard deviation as a function of iteration step for:  
 a) x-component of wind; b) y-component of wind; c) temperature;  
 d) specific humidity.

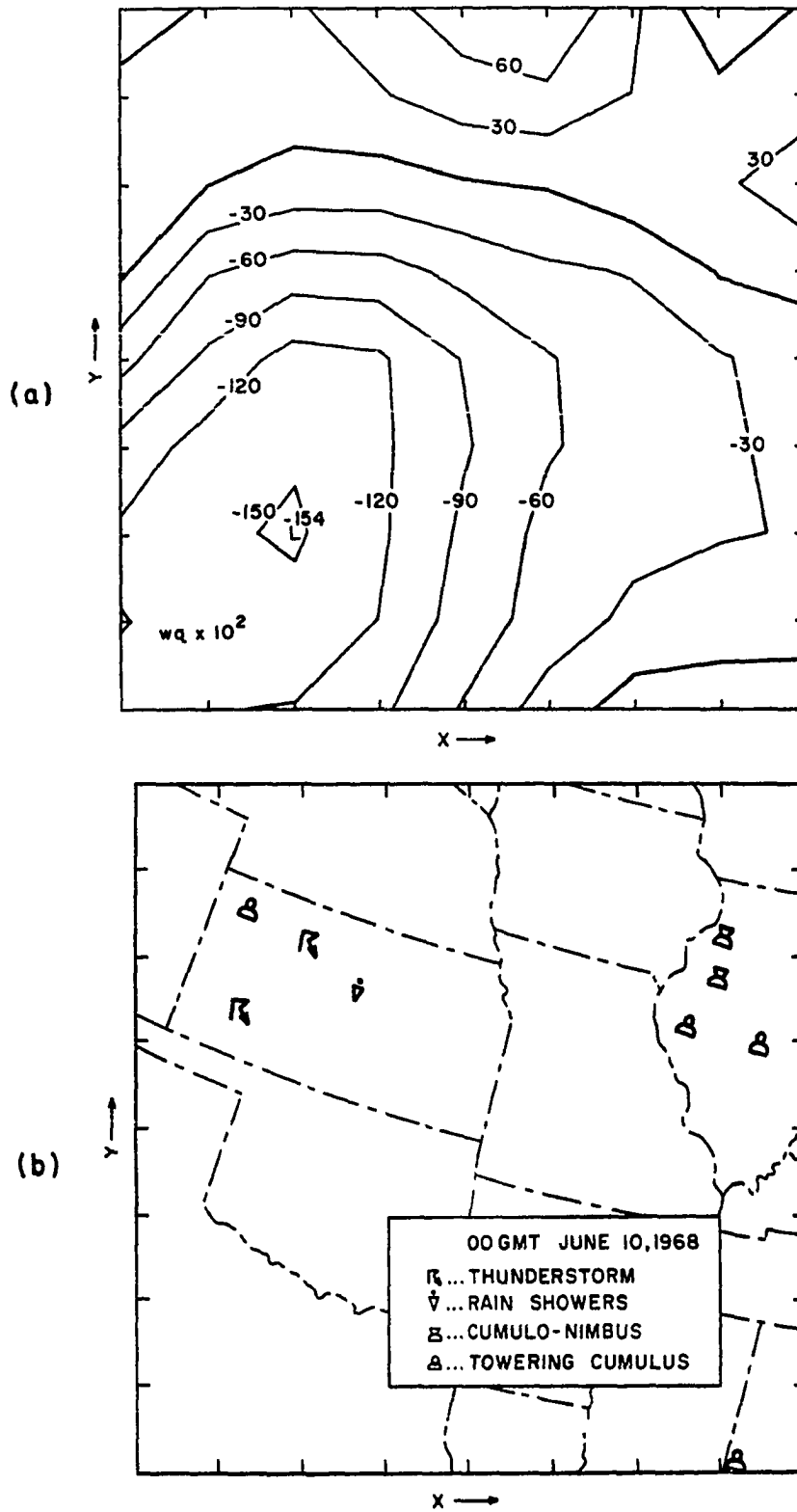


Fig. 7. 00 GMT, June 10,  $t = 0$ : 1) mid-level distribution of  $wq$ , non-dimensional severe storm index; 2) surface observations of severe weather.

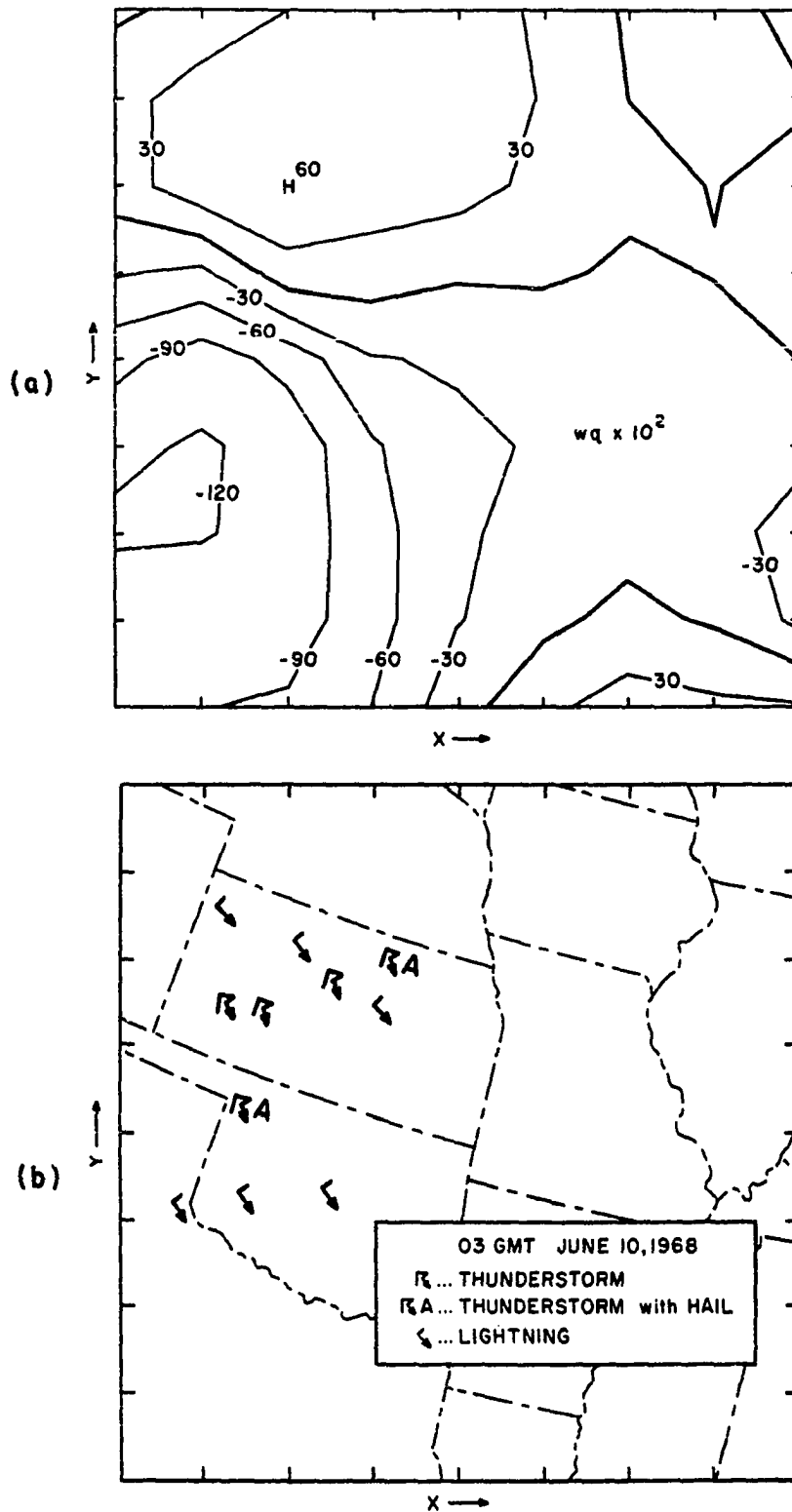


Fig. 8. 03 GMT, June 10,  $t = 3$  hr: a) mid-level distribution of  $wq$ , non-dimensional severe storm index; b) surface observations of severe weather.

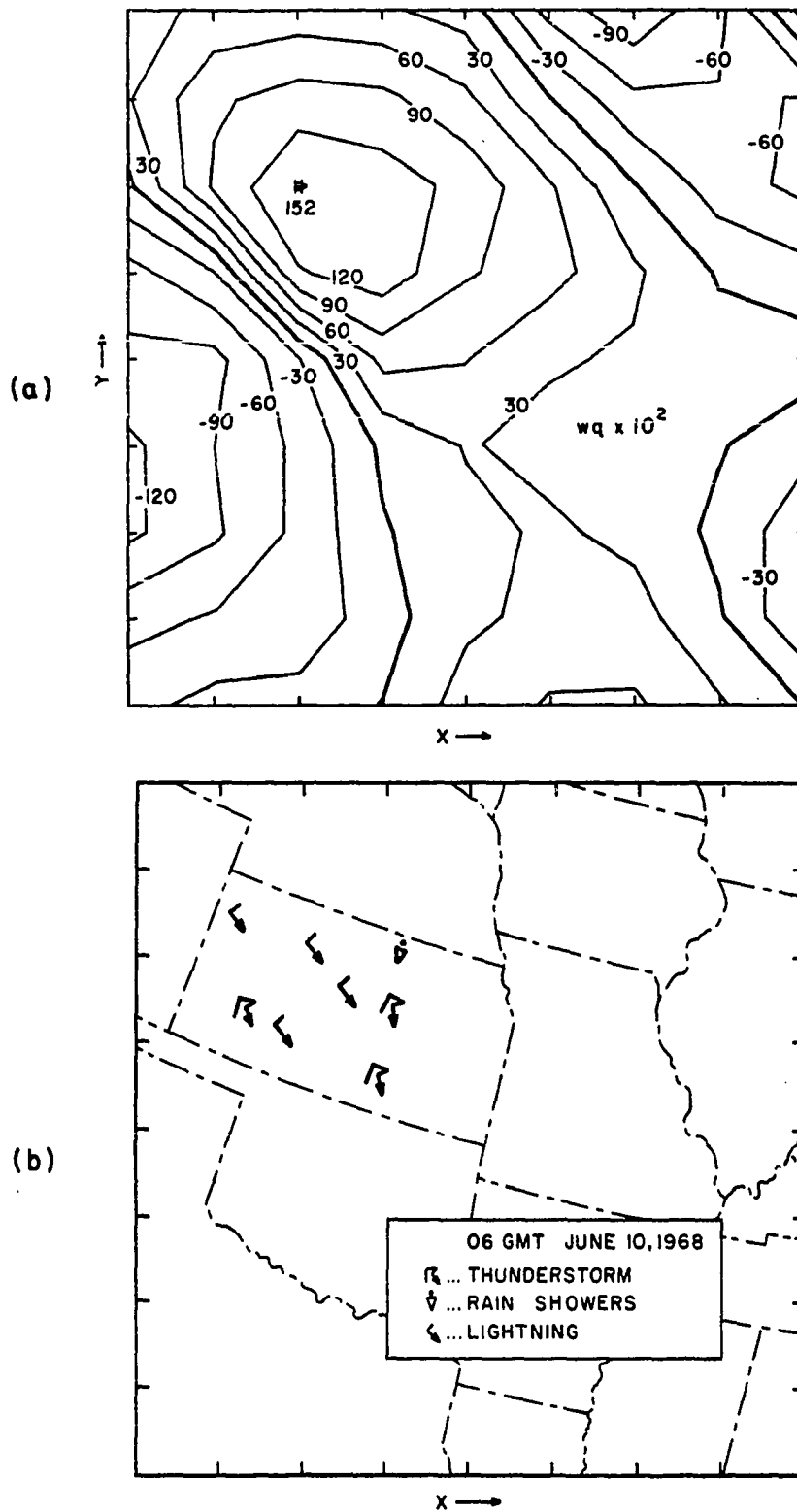


Fig. 9. 06 GMT, June 10,  $t = 6$  hr: a) mid-level distribution of  $wq$ , non-dimensional severe storm index; b) surface observations of severe weather.

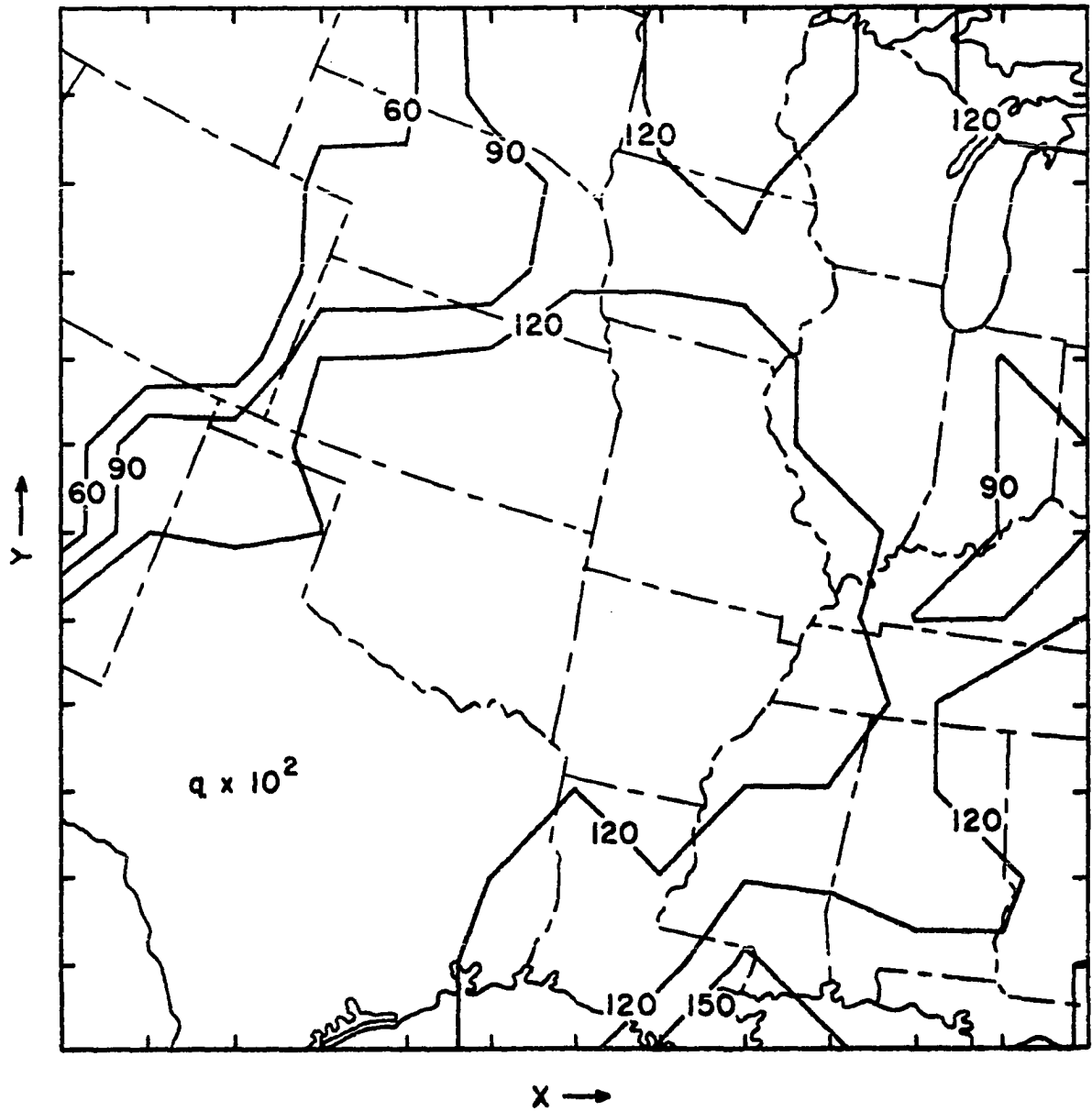


Fig. 10. 00 GMT, June 10,  $t=0$ : mid-level distribution of non-dimensional specific humidity,  $q$ .

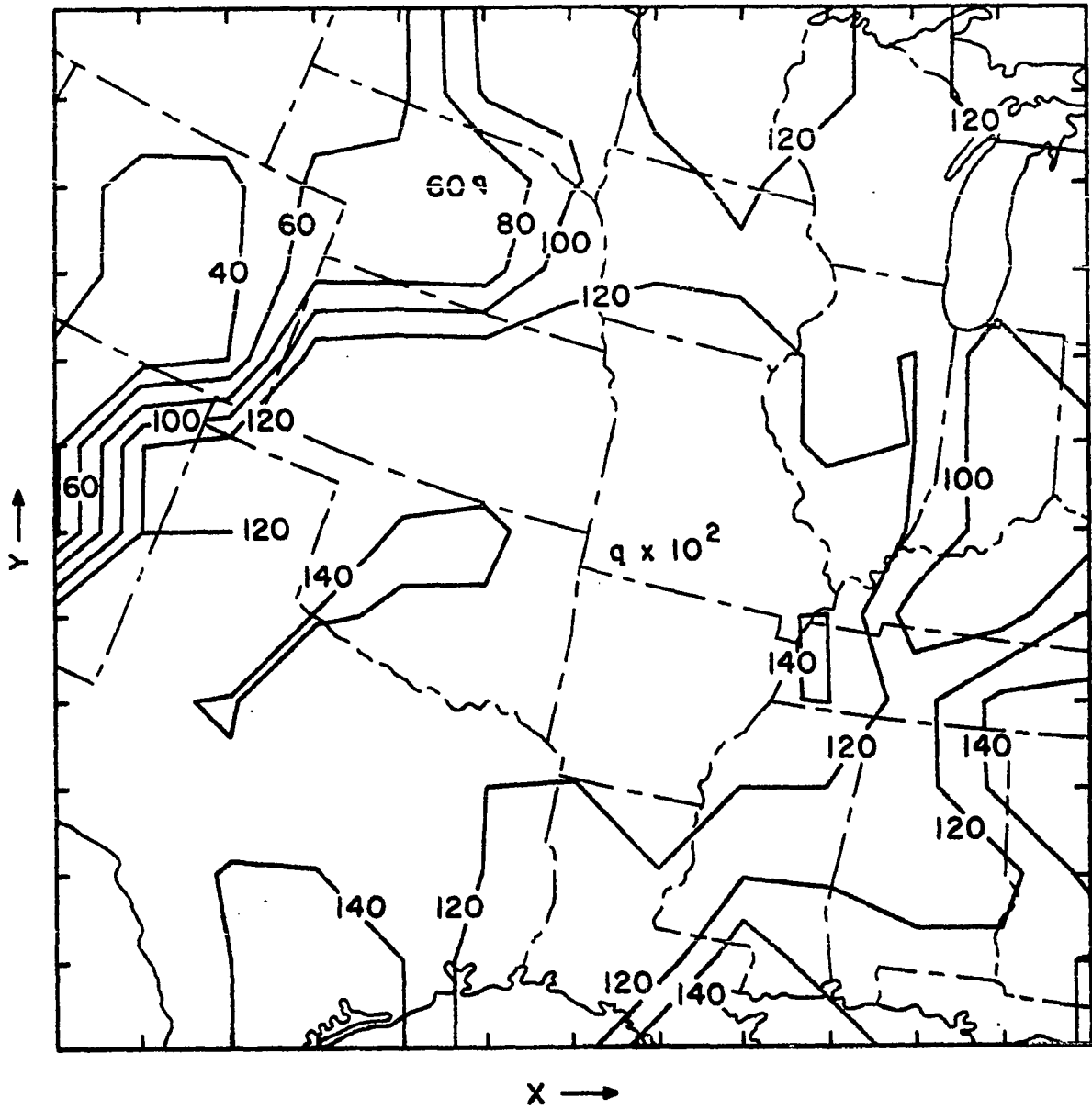


Fig. 11. 03 GMT, June 10,  $t = 3$  hr: mid-level distribution of non-dimensional specific humidity,  $q$ .

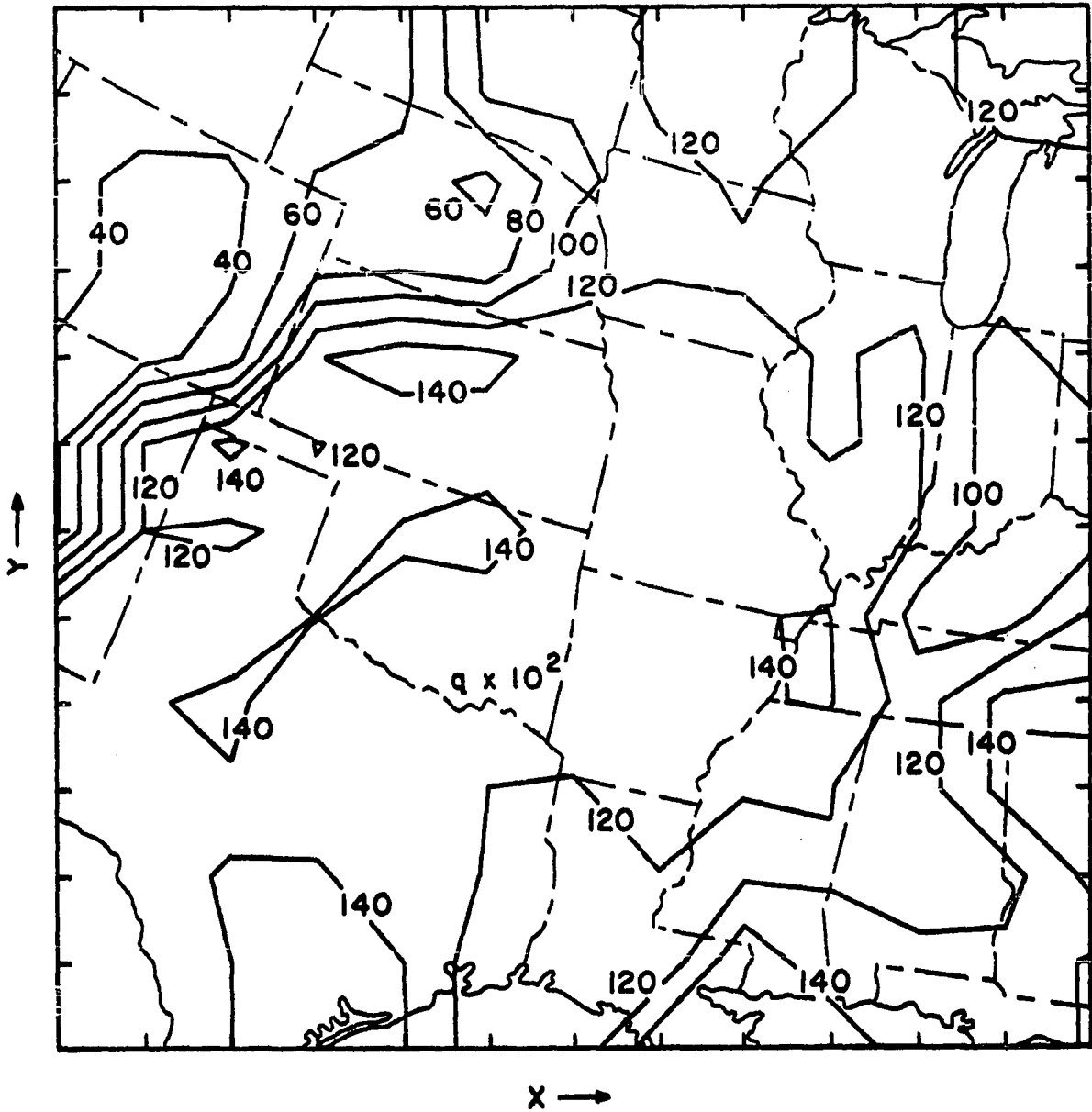


Fig. 12. 06 GMT, June 10,  $t = 6$  hr: mid-level distribution of non-dimensional specific humidity,  $q$ .

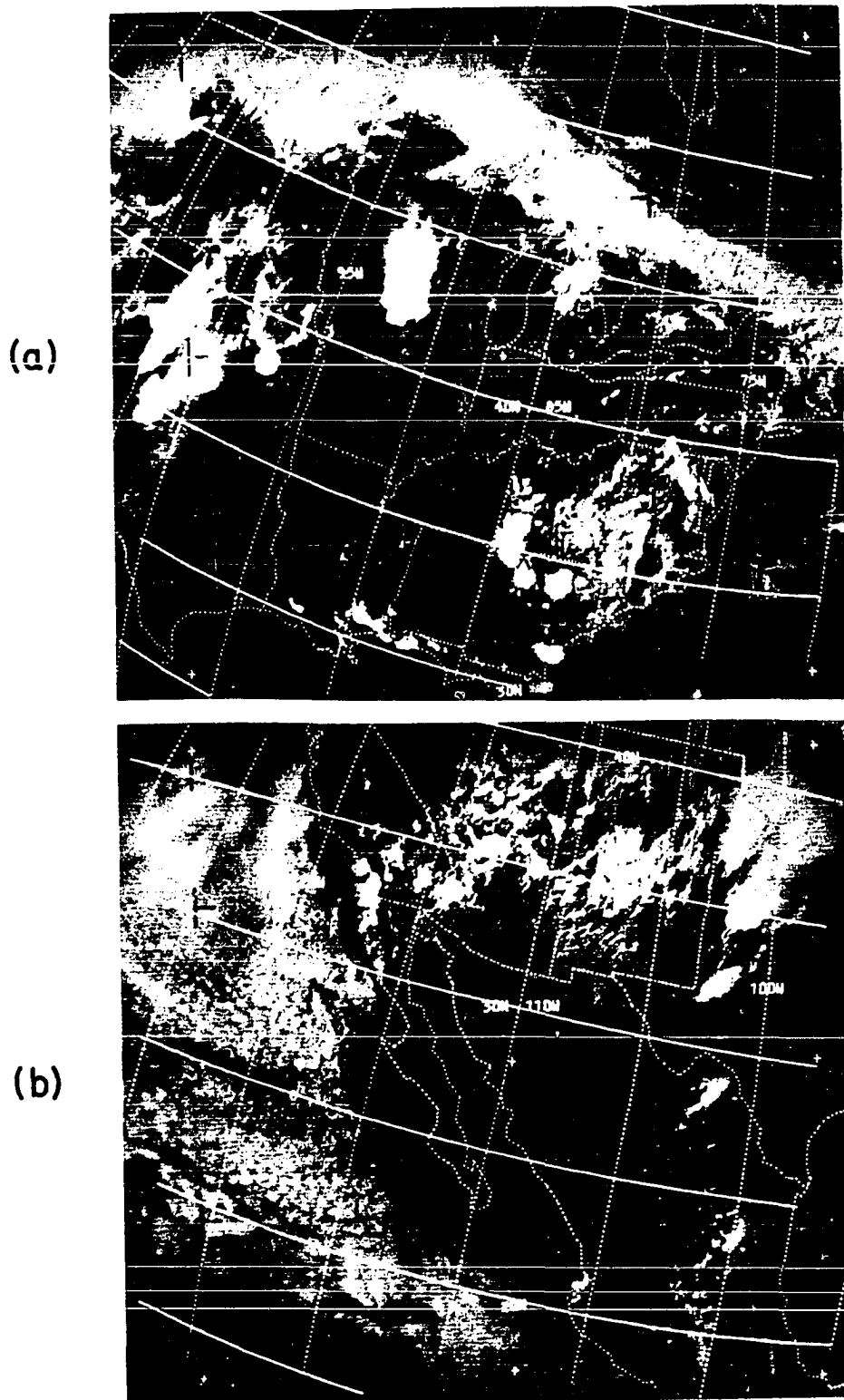


Fig. 13. ESSA-5 satellite photographs taken at: a) 2129 GMT, June 9,  $t \pm -2.5$  hr; b) 2318 GMT, June 9,  $t \pm -0.7$  hr.

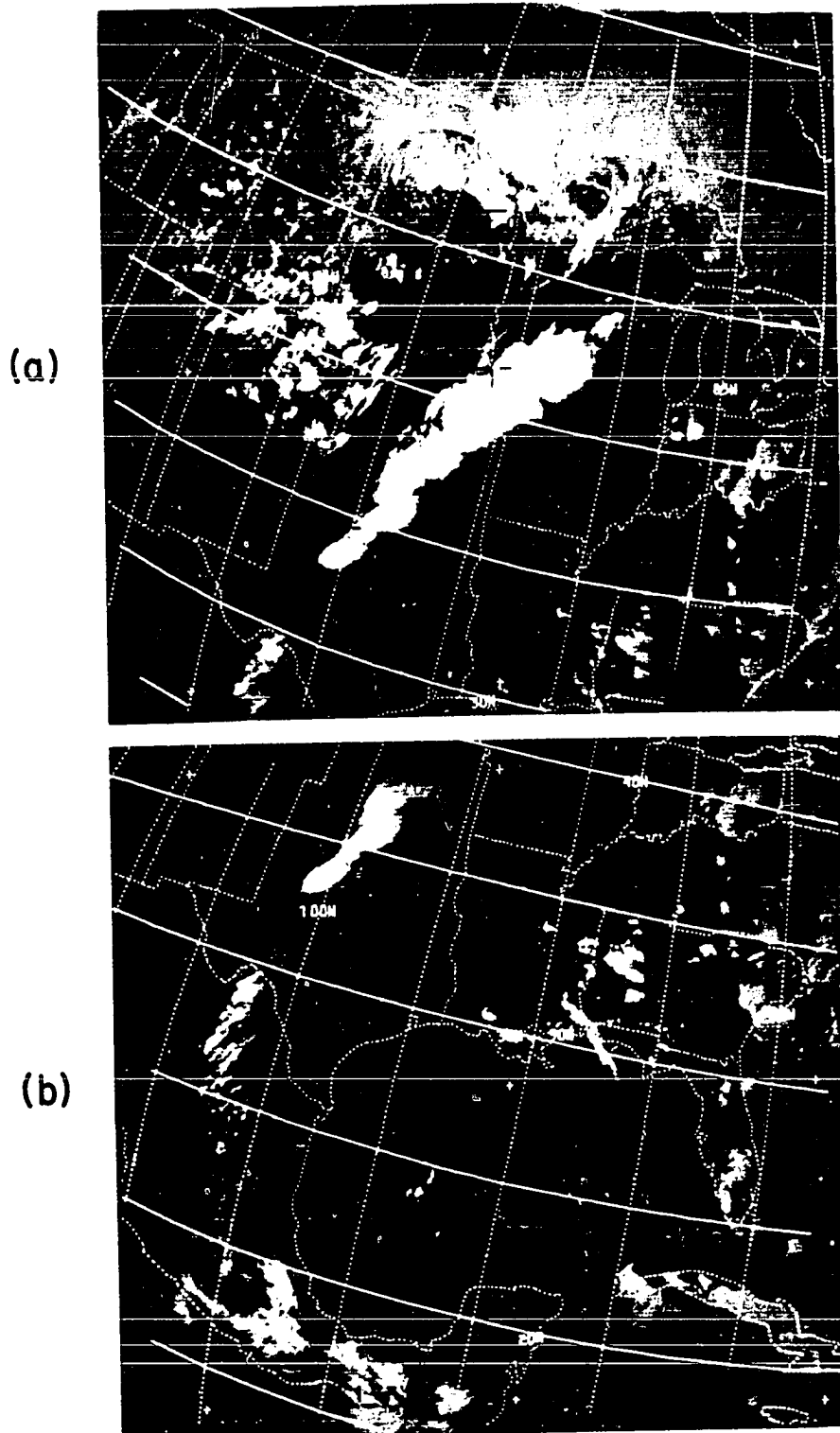


Fig. 14. ESSA-5 satellite photographs taken at: a) 2205 GMT, June 10,  $t \pm 22$  hr; b) 2201 GMT, June 10,  $t \pm 22$  hr.